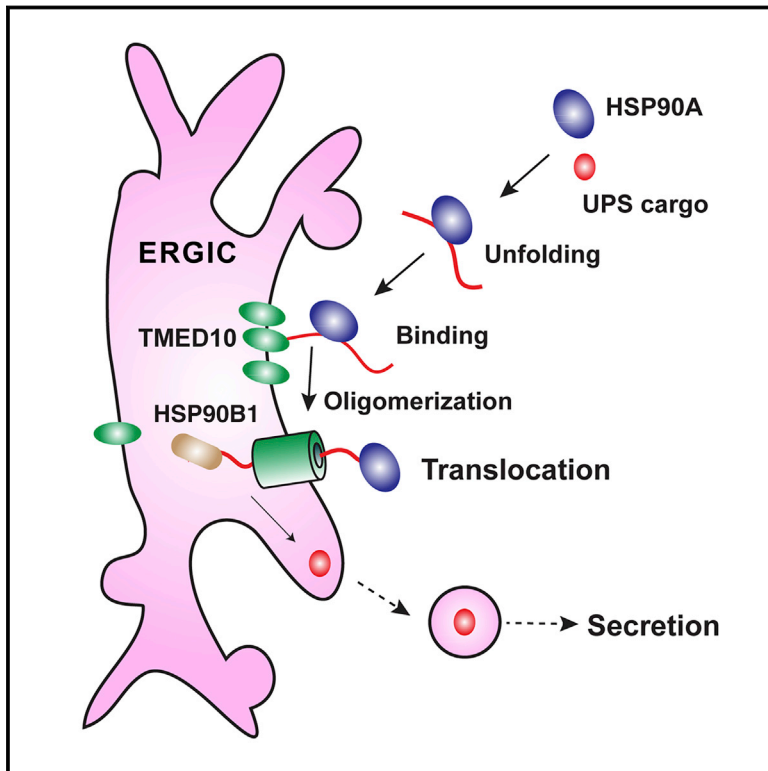


A Translocation Pathway for Vesicle-Mediated Unconventional Protein Secretion

Graphical Abstract



Authors

Min Zhang, Lei Liu, Xubo Lin, ...,
Xiachen Lv, Li Zheng, Liang Ge

Correspondence

liangge@mail.tsinghua.edu.cn

In Brief

On-demand secretion of inflammatory factors like IL-1 β and other protein cargoes lacking secretion signal sequences relies on TMED10, a protein that oligomerizes to channel the cargoes into secretory vesicles.

Highlights

- TMED10 regulates the secretion of a broad spectrum of cytosolic UPS cargoes
- TMED10 mediates the translocation of UPS cargoes into the vesicle
- TMED10 facilitates UPS cargo entry into the ER-Golgi intermediate compartment
- UPS cargo promotes TMED10 oligomerization for protein translocation

A Translocation Pathway for Vesicle-Mediated Unconventional Protein Secretion

Min Zhang,^{1,3} Lei Liu,^{1,3} Xubo Lin,² Yang Wang,¹ Ying Li,¹ Qing Guo,¹ Shulin Li,¹ Yuxin Sun,¹ Xuan Tao,¹ Di Zhang,¹ Xiachen Lv,¹ Li Zheng,¹ and Liang Ge^{1,4,*}

¹State Key Laboratory of Membrane Biology, Tsinghua University-Peking University Joint Center for Life Sciences, School of Life Sciences, Tsinghua University, Beijing 100084, China

²Beijing Advanced Innovation Center for Biomedical Engineering, Beihang University, Beijing 100191, China

³These authors contributed equally

⁴Lead Contact

*Correspondence: liangge@mail.tsinghua.edu.cn

<https://doi.org/10.1016/j.cell.2020.03.031>

SUMMARY

Many cytosolic proteins lacking a signal peptide, called leaderless cargoes, are secreted through unconventional secretion. Vesicle trafficking is a major pathway involved. It is unclear how leaderless cargoes enter into the vesicle. Here, we find a translocation pathway regulating vesicle entry and secretion of leaderless cargoes. We identify TMED10 as a protein channel for the vesicle entry and secretion of many leaderless cargoes. The interaction of TMED10 C-terminal region with a motif in the cargo accounts for the selective release of the cargoes. In an *in vitro* reconstitution assay, TMED10 directly mediates the membrane translocation of leaderless cargoes into the liposome, which is dependent on protein unfolding and enhanced by HSP90s. In the cell, TMED10 localizes on the endoplasmic reticulum (ER)-Golgi intermediate compartment and directs the entry of cargoes into this compartment. Furthermore, cargo induces the formation of TMED10 homo-oligomers which may act as a protein channel for cargo translocation.

INTRODUCTION

Over evolution, both eukaryotes and prokaryotes have acquired protein secretion as a fundamental mechanism for intercellular communication. In eukaryotes, the majority of secretory proteins contain a signal peptide that allows for signal recognition particle (SRP) binding followed by translocation of the cargo into the endoplasmic reticulum (ER) via the translocon SEC61 (Rapoport et al., 2017; Shan and Walter, 2005; Voorhees and Hegde, 2016). The cargoes are then exported through ER-Golgi trafficking mediated by COPII and COPI vesicles (Pantazopoulou and Glick, 2019; Zanetti et al., 2011). The overall process is termed as conventional secretion.

Recent studies found that many cytosolic proteins lacking a signal peptide (leaderless cargoes) are released through unconventional protein secretion (UPS) that bypasses the ER-Golgi trafficking itinerary (Nickel and Rabouille, 2009; Rabouille et al., 2012).

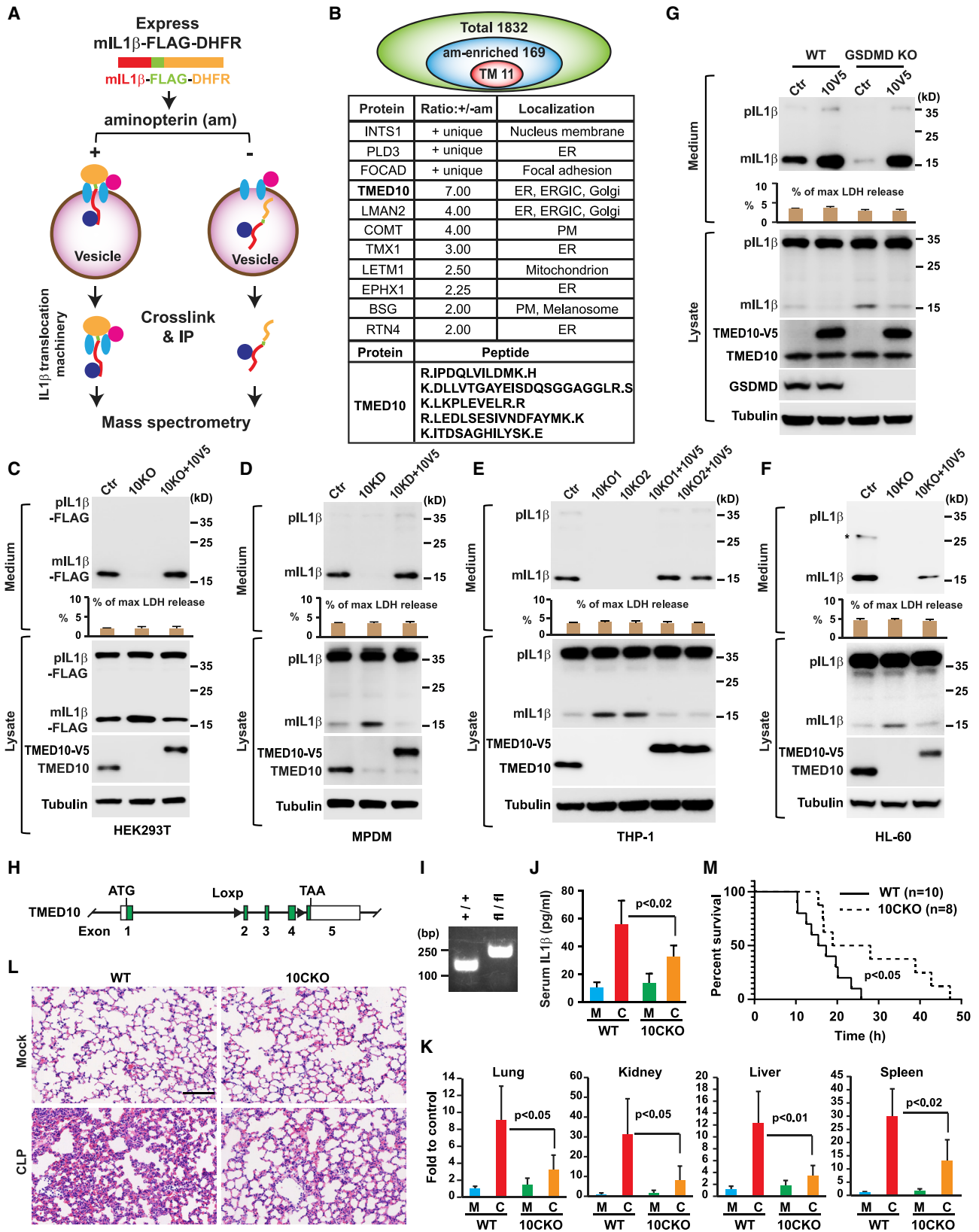
Expanding evidence indicates that cargoes that undergo UPS are involved in diverse biological processes (including inflammation, development, virus infection, and lipid metabolism) and human diseases (such as neurodegeneration and cancer) (Claude-Taupin et al., 2017; Dimou and Nickel, 2018; Ejlerskov et al., 2013; Lock et al., 2014; Malhotra, 2013; Rabouille, 2017; Villeneuve et al., 2018). Unlike a unified route for conventional secretion, UPS employs multiple means of protein delivery (Dimou and Nickel, 2018; Rabouille, 2017; Zhang and Schekman, 2013). Regarding the secretion of cytosolic UPS cargoes, two major mechanisms have been proposed. One mechanism involves direct protein penetration across the plasma membrane (PM) (type I unconventional secretion, e.g., fibroblast growth factor 2 [FGF2]) (Schäfer et al., 2004; Stinger and Nickel, 2018). The other mechanism is dependent on vesicular trafficking (type III unconventional secretion, e.g., yeast Acb1) (Duran et al., 2010; Malhotra, 2013). In the latter, the cargoes enter into a vesicle carrier that exports them through membrane trafficking. Because the cargoes lack a signal peptide, a key question has been how the leaderless cargoes enter into the vesicle carrier.

Here, we find a protein translocation pathway regulating leaderless cargo entry into the vesicle carrier in UPS. We identified a transmembrane protein transmembrane emp24 domain-containing protein 10 (TMED10)/TMP21 as a regulatory factor for the secretion of multiple cargoes, including the mature form of interleukin 1(IL-1) family members and a set of other UPS cargoes (HSPB5, galectin-1/3, Tau, and annexin A1). We found that TMED10 directly facilitates the translocation of leaderless cargos into the ER-Golgi intermediate compartment (ERGIC) via its C-terminal tail binding to a certain motif in the cargoes, the process of which is dependent on protein unfolding and enhanced by chaperones HSP90A/HSP90AB1 and HSP90B1/GRP94. Furthermore, the cargo triggers oligomerization of TMED10, which likely then forms a protein channel on the membrane to translocate the UPS cargoes into the vesicle.

RESULTS

TMED10 Is Required for the Secretion of Mature IL-1 β in Inflammatory and Non-inflammatory Cells

IL-1 β is a most intensely investigated UPS cargo that undergoes type I and type III pathways (Claude-Taupin et al., 2018; Dimou



(legend on next page)

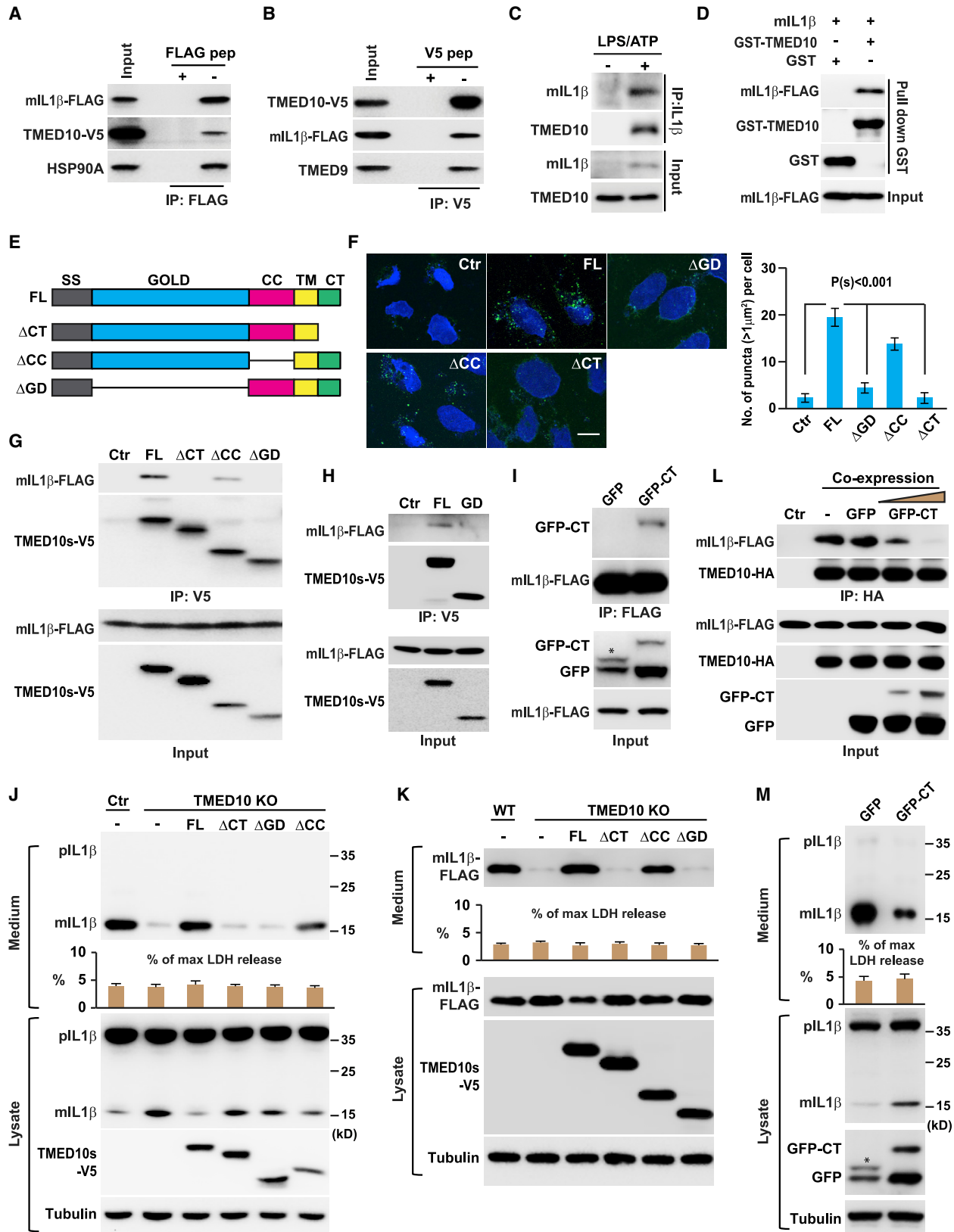
and Nickel, 2018; Rubartelli et al., 1990; Sitia and Rubartelli, 2018). In the type I pathway, IL-1 β is released through a pore formed by the N-terminal fragment of gasdermin D (GSDMD) on the PM (Evavold et al., 2018; Kayagaki et al., 2015; Shi et al., 2015). In the type III pathway, IL-1 β transits through vesicular carriers, including secretory lysosomes, autophagosomes, and multivesicular bodies (Dupont et al., 2011; Schatz and Dobberstein, 1996; Semino et al., 2018; Verhoef et al., 2003; Zhang et al., 2015). The data from both others and us have indicated that the mature IL-1 β (mIL-1 β) is translocated into a vesicle carrier (Andrei et al., 1999; Dupont et al., 2011; Semino et al., 2018; Zhang et al., 2015). In addition, we found that the translocation is dependent on protein unfolding, which implicates the involvement of a translocon-like protein channel (Zhang et al., 2015). In order to identify the protein channel accounting for mIL-1 β translocation, we employed a dihydrofolate reductase (DHFR) system coupled with protein crosslink and mass spectrometry (Figure 1A). Because aminopterin inhibits DHFR unfolding (Andrei et al., 1999; Backhaus et al., 2004), the folded DHFR will likely plug the DHFR-tagged mIL-1 β on the translocation machinery. This allows us to enrich the translocation machinery that associates with mIL-1 β in the presence of aminopterin (Figure 1A). A semiquantitative mass spectrometry analysis identified 169 proteins that were more than 2-fold enriched or unique in the aminopterin-treated group. Of the 169 proteins, 11 were transmembrane proteins (Figure 1B; Table S1). We silenced the expression of the candidates by small hairpin RNAs (shRNAs) and found that knockdown (KD) of TMED10 decreased mIL-1 β secretion (Figures S1A and S1B). We confirmed the requirement of TMED10 for mIL-1 β secretion by creating three TMED10 CRISPR knockout (KO) cell lines (Figure S1C). Exogenous expression of TMED10 increased mIL-1 β secretion, whereas LMAN2 (another transmembrane protein candidate) expression showed no effect (Figure S1D). In addition, the requirement of TMED10 on IL-1 β secretion is mature form specific (Figure 1C).

IL-1 β is mainly released by inflammatory cells, such as macrophages and neutrophils (Sitia and Rubartelli, 2018). To determine the requirement of TMED10 for mIL-1 β secretion in macrophages, we employed two differentiated macrophage cell lines, the mouse myeloid progenitor-derived macrophage (MPDM) (Figure 1D) and THP-1-differentiated macrophage (Figure 1E). In both cell lines, depletion of TMED10 via lentivirus-mediated RNAi (Figure 1D) or CRISPR KO (Figure 1E) dramatically reduced mIL-1 β secretion, which was restored by re-expression of TMED10 (Figures 1D and 1E). A similar effect was also observed in a differentiated neutrophil-like cell line HL-60 (Figure 1F). In an IL-1 β reporter assay, the secreted alkaline phosphatase (SEAP) activity corresponded to the level of mIL-1 β in the medium from each TMED10-modulated cell (Figures S1E–S1G), which indicates that TMED10 regulates the secretion of active mIL-1 β in both inflammatory and non-inflammatory cells. It has been shown that the activated form of caspase-1 was also released under conditions that stimulate IL-1 β secretion (Albus et al., 2012; He et al., 2015; Qu et al., 2007; Schneider et al., 2012). The release of p20, a subunit of the activated caspase-1, was not affected by TMED10 KO (Figure S1H), suggesting that TMED10 is not involved in caspase-1 release.

GSDMD cleavage-mediated pore formation and pyroptosis was recently shown to induce massive release of IL-1 β in macrophages (Evavold et al., 2018; Kayagaki et al., 2015; Shi et al., 2015). Expression of TMED10 increased IL-1 β secretion in GSDMD-KO THP-1 with similar extent to the wild-type (WT) THP-1, although GSDMD KO reduced IL-1 β release without TMED10 expression (Figure 1G). Further, GSDMD KO did not affect the TMED10-regulated secretion of mIL-1 β in non-inflammatory cells (Figure S1I). Another study indicated the possibility of mIL-1 β release through directly penetrating the PM via binding to PIP2 and destabilizing the lipid bilayer (Monteleone et al., 2018). The TMED10-promoted mIL-1 β secretion was not affected by the PM lipid-stabilizing reagent punicalagin or

Figure 1. TMED10 Regulates IL-1 β Secretion

- (A) Diagram showing isolation of the membrane protein complex associating with mIL-1 β . Cells expressing mIL-1 β -FLAG-DHFR were incubated with (+) or without (–) aminopterin (am) followed by DSP crosslink. The membrane fractions were collected followed by immunoprecipitation to isolate the mIL-1 β membrane protein complexes. Mass spectrometry was employed to identify peptides enriched in each complex.
- (B) Venn diagram and tables showing transmembrane membrane proteins enriched in am (+) and the identified peptides of TMED10.
- (C) IL-1 β secretion in WT or TMED10-KO HEK293T with or without TMED10-V5 expression transfected with plasmids of the mature (m) and precursor (p) IL-1 β . Bars indicate LDH release (mean \pm SD).
- (D) IL-1 β secretion in mouse myeloid progenitor cells infected with lentiviruses containing control (Ctr) shRNAs or TMED10 shRNAs with or without TMED10-V5(10V5) re-expression. The cells were differentiated, primed with 100 ng/mL LPS overnight, and treated with 1.5 mM ATP for 30 min. Bars indicate LDH release (mean \pm SD).
- (E) IL-1 β secretion in WT and two TMED10 KO (10KO) THP-1 generated by CRISPR-CAS9 with or without TMED10-V5 (10V5) re-expression. The cells were differentiated and treated with LPS followed by ATP. Bars indicate LDH release (mean \pm SD).
- (F) IL-1 β secretion in control or TMED10 KO HL-60 with or without TMED10-V5 re-expression. The cells were differentiated by 1.3% DMSO for 6 days and treated with LPS followed by ATP. Bars indicate LDH release (mean \pm SD). *Non-specific band.
- (G) IL-1 β secretion in control or GSDMD KO THP-1 with or without TMED10-V5 expression (10V5). Bars indicate LDH release (mean \pm SD).
- (H) Scheme of TMED10 KO mice generation. The loxp was placed before exon 2 and after exon 4. Expression of Cre leads to the deletion of exons 2–4.
- (I) PCR validation of mice without (+/+) or with loxp insertion (fl/fl).
- (J) 6 h after mock (M) or CLP (C) surgery, the mice were sacrificed and serum IL-1 β level were determined by ELISA (mean \pm SD). p value is indicated (two-tailed t test, n = 6).
- (K) 6 h after mock (M) or CLP (C) surgery, the mice were sacrificed and the expression level of IL6 in indicated tissues were analyzed (mean \pm SD). p values are indicated (two-tailed t test, n = 6).
- (L) Similar surgery was performed as indicated in (J) and (K). After 12 h, the lungs were collected followed by H&E staining. Representative sections were shown. Scale bar, 100 μ m
- (M) CLP surgery was performed as indicated above and survival curves of WT and KO mice (10CKO) were recorded. p and n were indicated.



(legend on next page)

mutating the PIP2-binding polybasic motif of mL-1 β in our system (Figures S1J and S1K). Together, the data suggest that TMED10 facilitates mL-1 β secretion independent of GSDMD or PM penetration.

TMED10 Regulates Serum IL-1 β Level and Inflammation in a Mice Model of CLP-Induced Septic Shock

It was shown that whole-body TMED10-KO mice were not viable (Denzel et al., 2000). To determine a role of TMED10 in regulating IL-1 β secretion in physiological settings, we generated TMED10-Loxp mice and crossed with Lyz2-Cre mice to create myeloid cell lineage-specific TMED10 conditional knockout mice (CKO) (Figures 1H and 1I). In a model of cecal ligation and puncture (CLP)-induced septic shock (Lu et al., 2019; Ruiz et al., 2016), TMED10 CKO, compared to WT, led to compromised IL-1 β rise in the serum and correspondingly less production of IL-6, an effector of IL-1 β (Mantovani et al., 2019), in the lung, kidney, liver, and spleen (Figures 1J and 1K). In addition, compared to WT littermates, injury of the lung caused by the septic shock was largely reduced in TMED10 CKO mice, and consistently the survival time was increased (Figures 1L and 1M). The data suggest that TMED10 regulates IL-1 β release and inflammation physiologically.

TMED10 Associates with mL-1 β via the C-Terminal Region

TMED10 associated with mL-1 β in co-immunoprecipitations (coIPs) (Figures 2A and 2B). As positive controls, mL-1 β or TMED10 associate with HSP90A or TMED9, respectively (Figures 2A and 2B), which is consistent with the previous data (Füllkrug et al., 1999; Zhang et al., 2015). Endogenous TMED10 and mL-1 β associated in lipopolysaccharide (LPS) and ATP-stimulated THP-1 cells and the interaction is direct as evidenced by an *in vitro* GST pull-down assay (Figures 2C, 2D, and S2A–S2C [protein gel]). We did not detect an association between TMED10 and caspase-1 (Figure S1L).

TMED10 is a membrane protein with a single transmembrane domain, a luminal part containing a signal peptide (SS), a GOLD domain and a coil-coil (CC) domain, as well as a C-terminal tail (CT) facing the cytoplasm (Figure 2E) (Pastor-Cantizano et al.,

2016). We constructed plasmids expressing domain deletion mutants. In both coIP and Duolink PLA, TMED10 truncations with the GOLD or CT deletion failed to associate with mL-1 β (Figures 2F and 2G), indicating that the two parts are responsible for mL-1 β interaction. To find the direct interaction part, we performed coIP of mL-1 β with the GOLD or the CT. The GOLD failed to associate with mL-1 β whereas the CT did, indicating that the CT directly interacts with mL-1 β (Figures 2H and 2I).

To determine the role of TMED10-mL-1 β interaction, we re-expressed the full-length TMED10 and each truncation in TMED10-KO cells. Consistent with the protein interaction assay, deletion of the GOLD or the CT failed to rescue mL-1 β secretion in both inflammatory and non-inflammatory cells (Figures 2J and 2K). To further confirm the functional significance of the TMED10-mL-1 β interaction, we overexpressed the TMED10-CT construct, which competed against TMED10-mL-1 β interaction and consequently blocked mL-1 β secretion (Figures 2L and 2M).

TMED10 Facilitates the Secretion of a Broad Spectrum of UPS Cargoes

To determine if TMED10 plays a broader role in unconventional secretion, we determined the effect of TMED10 on the secretion of the mature form of IL-1 family members (that lack signal peptides and have been suggested to undergo UPS) and a set of other reported UPS cargoes (Chauhan et al., 2013; Claude-Taupin et al., 2017; Dimou and Nickel, 2018; Dinarello, 2018; Ejlerskov et al., 2013; Gardella et al., 2002; Malhotra, 2013; Mantovani et al., 2019; Popa et al., 2018). Of the UPS cargoes tested, KD of TMED10 decreased the secretion of the mature forms of IL-1 family members and other cargoes including HSPB5, galectin-1/3, annexin A1, and Tau, but not high mobility group box 1 (HMGB1) or α -synuclein (Figures 3A, S3A, and S3B). As controls, two type I UPS cargoes (FGF2 and HIV-TAT) and conventional secretion cargoes (ssGFP and IL-6) were not affected by TMED10 depletion (Figures 3A, S3A, and S3B).

The above interaction analysis indicates that TMED10 regulates the secretion of mL-1 β via association with its CT (Figure 2I). To determine the role of the TMED10-CT in regulating the secretion of the cargoes, we analyzed the effect of

Figure 2. TMED10 Interacts with IL-1 β

(A) CoIP using HEK293T with mL-1 β -FLAG and TMED10-V5 expression using anti-FLAG agarose with or without FLAG peptide.

(B) CoIP using HEK293T shown in (A) with anti-V5 agarose with or without V5 peptide.

(C) CoIP with anti-IL-1 β antibody using THP-1 primed for IL-1 β secretion.

(D) GST pull down analysis using GST, GST-TMED10, and mL-1 β proteins.

(E) Diagram showing the truncation constructs of TMED10-V5. Signal peptide (SS), aa 1–31; GOLD domain, aa 32–132; coil-coil domain (CC), aa 133–185; transmembrane domain (TM), aa 186–206; C-terminal (CT), aa 207–219.

(F) Duolink PLA assay performed with U2OS expressing TMED10-V5 alone (Ctr) or indicated TMED10-V5 variants with mL-1 β -FLAG (scale bar, 10 μ m). Quantification of the Duolink signal represents mean \pm SD. p values are indicated (two-tailed t test, n = 3).

(G) CoIP using HEK293T with mL-1 β -FLAG and indicated TMED10-V5 variants.

(H) CoIP using TMED10-KO HEK293T with mL-1 β -FLAG and TMED10 GOLD domain.

(I) CoIP using TMED10-KO HEK293T with mL-1 β -FLAG and GFP or GFP-tagged TMED10 C-terminal (GFP-10-CT). *An unknown modification of GFP that occurs occasionally.

(J) IL-1 β secretion in WT or TMED10-KO THP-1 re-expressing the indicated TMED10 variants. Bars indicate LDH release (mean \pm SD).

(K) Secretion of mL-1 β -FLAG in WT or TMED10-KO HEK293T re-expressing the indicated TMED10 variants. Bars indicate LDH release (mean \pm SD).

(L) The HEK293T cells were expressed with mL-1 β -FLAG, TMED10-HA, and GFP or increasing amount of GFP-10-CT. CoIP was performed using the above cells.

(M) THP-1 cells were expressed with GFP or GFP-tagged CT of TMED10 (GFP-CT) followed by differentiation and mL-1 β secretion determination. Bars indicate LDH release (mean \pm SD). *An unknown modification of GFP that occurs occasionally.

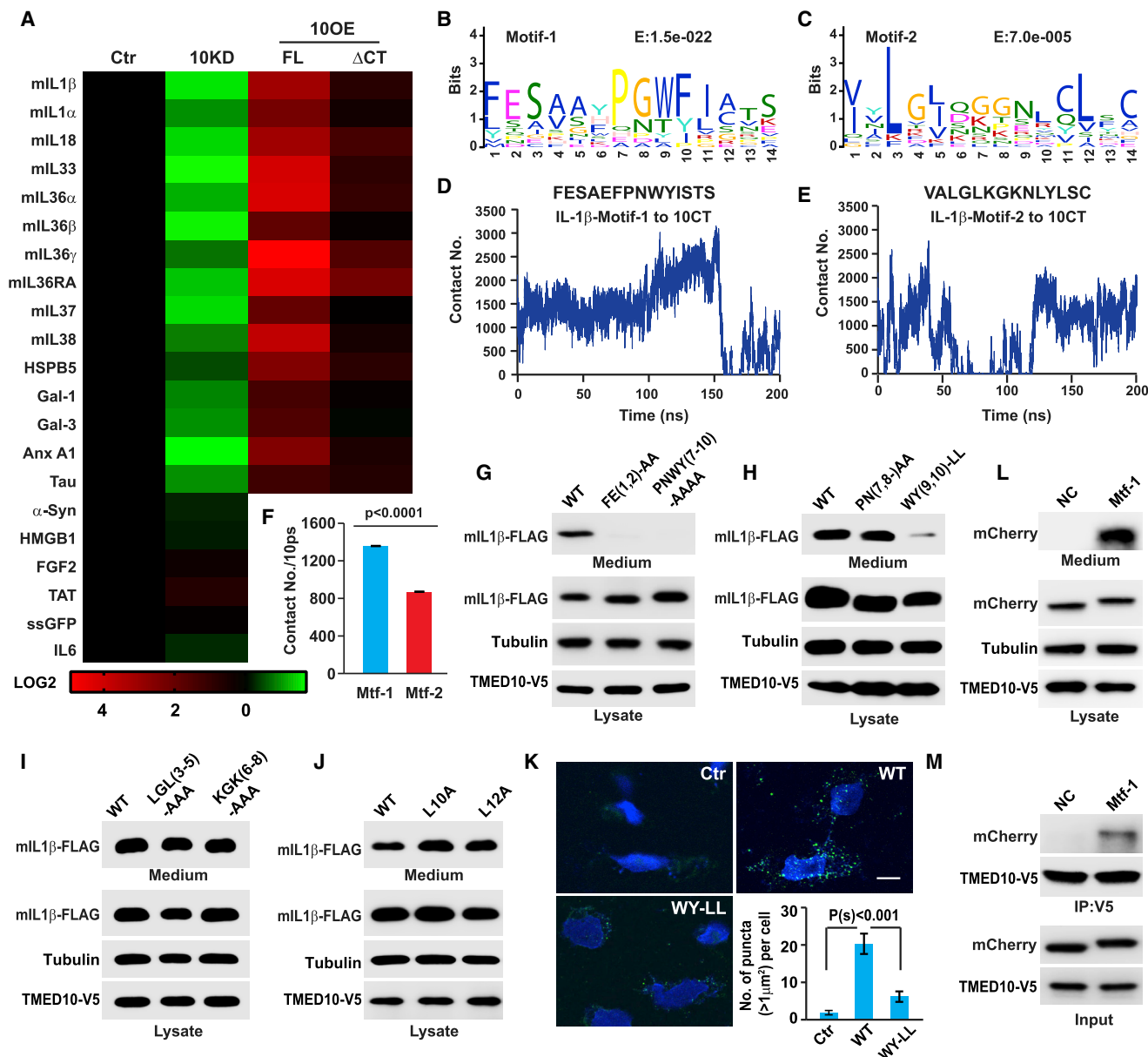


Figure 3. TMED10 Facilitates the Secretion of a Set of Unconventional Secretory Cargoes Dependent on Its C-Terminal Binding to a Certain Motif of the Cargo

(A) Heatmap showing the secretion of indicated unconventional secretory cargoes in TMED10 KD, full-length, or C-terminal deletion expression HEK293T cells. Cargo secretion in control cells was set as 1, and the secretion in TMED10 modulated cells were calculated relative to control cells. The heatmap shows the log₂ value.

(B and C) Two potential motifs, motif-1 (B) and motif-2 (C), predicted by MEME based on the sequence of 15 cargoes the secretion of which was regulated by TMED10 (with E value less than 0.05).

(D–F) Molecular dynamic simulation of the binding between TMED10-CT and motif-1 (D) or 2 (E) from IL-1β. Average binding events per 10 picoseconds are shown in (F). Bars indicate SEM. p value is indicated (two-tailed t test, n = 20,000).

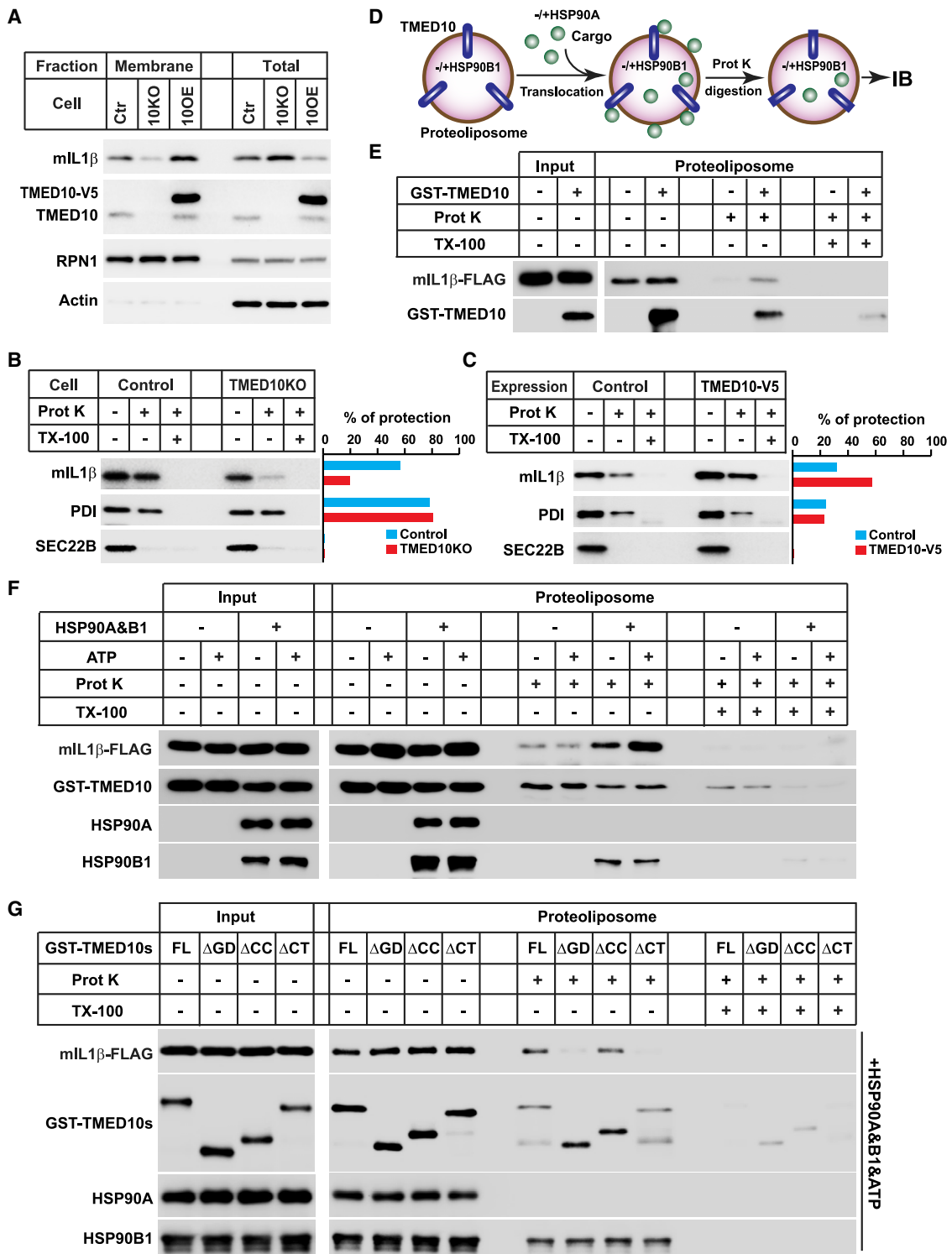
(G and H) Secretion of mIL-1β with indicated mutations in motif-1 (FE(1,2)-AA and PNWY(7-10)-AAAA in G, PN(7,8)-AA and WY(9,10)-AA in H) in HEK293T with TMED10 expression.

(I and J) Secretion of mIL-1β with indicated mutations in motif-2 (LGL(3-5)-AAA and KGK(6-8)-AAA in I, L10A and L12A in J) in HEK293T with TMED10 expression.

(K) Duolink PLA assay performed with U2OS expressing TMED10-V5 alone (Ctr) or TMED10-V5 with WT mIL-1β-FLAG or the WY-LL mutant respectively (scale bar, 10 μm). Quantification of the Duolink signal represent mean ± SD. p values are indicated (two-tailed t test, n = 3).

(L) Secretion of a cytosolic protein mCherry without or with motif-1 from IL-1β in HEK293T with TMED10 expression.

(M) CoIP of a cytosolic protein mCherry without or with motif-1 from IL-1β with TMED10.



TMED10 and TMED10-CT expression on the secretion of the cargoes relying on TMED10 for secretion (Figures 3A and S3C). Consistently, full-length TMED10 expression increased the secretion of these UPS cargoes whereas TMED10-CT showed compromised effect (Figures 3A and S3C). In colP, a majority of the cargoes associated with TMED10 in a CT-dependent manner (Figure S3D). Together, the data indicate that TMED10 regulates the secretion of a category of UPS cargoes dependent on its CT association with the cargoes. The association of annexin A1 or Tau with TMED10 was barely detectable in the colP assay (data not shown). It is likely that the interaction is too weak to be detected or TMED10 may indirectly regulate the secretion of annexin A1 and Tau.

It is possible that these UPS cargoes contain a common motif that directs them to the TMED10-regulated pathway for secretion. To look for such a sequence, we uploaded the sequences of these UPS cargoes in the MEME-Suite website for the discovery of common motifs (Bailey and Elkan, 1994). The website returned two motifs with an E value less than 0.05, which we named motif-1 and motif-2 (Figures 3B, 3C, S3E, and S3F). We performed molecular dynamics simulation to predict the binding between TMED10-CT and the two motifs on mL-1 β . Of the 200 ns (ns) simulation time, motif-1 showed a strong binding with TMED10-CT in the first 170 ns, whereas motif-2 displayed less stable association (Figures 3D–3F). Mutation of the highly common residues in mL-1 β motif-1 (positions 1, 2 [FE(1,2)-AA], 7–10 [PNWY(7–10)-AAAA], and 9, 10 [WY(9,10)-LL]) abolished the TMED10-promoted secretion, whereas similar mutations in motif-2 (positions 3–5 [LGL[3–5]-AAA], 6–8 [KKG(6–8)-AAA], 10[L10A], and 12[L12A]) showed marginal effect (Figures 3G–3J). The data together indicate that motif-1 is more likely to participate in TMED10-mediated UPS. Notably, WY(9,10)-LL mutation reduced mL-1 β -TMED10 association in a Duolink PLA assay, suggesting the requirement of motif-1 for the interaction (Figure 3K). To determine if motif-1 is sufficient to drive secretion, we fused mL-1 β motif-1 to an mCherry protein. The motif-1 containing mCherry was able to associate with TMED10 and be secreted whereas the mCherry alone was not (Figures 3L and 3M), indicating that motif-1 is sufficient to direct a leaderless cargo to the route of secretion.

TMED10 Directly Promotes the Membrane Translocation of Leaderless Cargoes

To determine the role of TMED10 in leaderless cargo entry into the vesicle, we performed membrane isolation and proteinase K protection (Figures 4A–4C) (Zhang et al., 2015). KO of TMED10 decreased the amount of mL-1 β in the membrane (Figure 4A). The residual mL-1 β on TMED10KO cell membrane was barely protected from proteinase K digestion compared to control cells (~3-fold decrease), indicating the deficiency of mL-1 β membrane entry without TMED10 (Figure 4B). On the contrary,

with exogenous TMED10 expression, the membrane fraction contained a higher level of mL-1 β that became more resistant to proteinase K digestion (~2-fold increase, Figures 4A and 4C). The data suggest that TMED10 facilitates mL-1 β entry into vesicles.

To test the direct involvement of TMED10 in cargo membrane entry, an *in vitro* membrane translocation assay was performed (Figure 4D). We purified TMED10 and incorporated it into liposomes (Figure 4D). In a flotation assay, the TMED10 protein stayed with the membrane after treatment with 2 M Urea or Na₂CO₃ (PH:11), indicating that TMED10 is integrated into the membrane (Figure S2D). A proteinase K protection assay showed that around half of the TMED10 with the CT facing outside on the liposome, which is the correct topology for the outside-in translocation assay (Figure S2E). The presence of TMED10 in the liposome generated a fraction of mL-1 β protected from proteinase K digestion compared to the control liposome (Figure 4E), which is TMED10 dose-dependent and temperature-dependent (Figures S4A and S4B), indicating that mL-1 β enters into the vesicle through TMED10. Similar translocation assays were performed with mL-18, mL-33, mL-36 α , and mL-37 that also showed a TMED10-dependent vesicle entry (Figures S4D–S4G).

The previous studies reported a requirement of HSP90 in IL-1 β membrane entry and secretion (Zhang et al., 2015; Zhang et al., 2018b). HSP90A and HSP90B1, the two HSP90s located in the cytosol and ER lumen, respectively, directly interacted with mL-1 β (Figures S2 [protein gel], S5A, and S5B) and regulated mL-1 β secretion (Figures S5C and S5D). HSP90s, when combined together, boosted the translocation of mL-1 β in an ATP-dependent manner (Figures 4F and S5E). The data indicate that TMED10, together with HSP90A and HSP90B1, directly facilitates mL-1 β membrane translocation.

The aforementioned data demonstrated the requirement of mL-1 β binding in TMED10-mediated leaderless cargo secretion. Consistently, the GOLD- or CT-truncated TMED10 mutant lost its ability to promote the membrane translocation of mL-1 β (Figure 4H). Together, the data indicate that TMED10 is a sufficient and direct factor for membrane translocation of the UPS cargoes.

Cargo Unfolding Regulates TMED10-Mediated Translocation

Previously, we found that IL-1 β unfolding is required for its membrane entry and secretion (Zhang et al., 2015). To determine if cargo unfolding is required for TMED10-mediated translocation, we incorporated the DHFR-aminopterin system shown above into the translocation assay. Aminopterin abolished the TMED10-dependent membrane entry of mL-1 β -DHFR in the conditions of both with and without HSP90s, confirming that protein unfolding is required for cargo translocation (Figure 5A and S4C).

(D) Diagram of *in vitro* translocation assay. In brief, GST-TMED10 proteoliposomes without or with HSP90B1 in the lumen were incubated with a purified cargo alone or with HSP90A. Proteinase K digestion was performed to determine the amount of membrane incorporated mL-1 β .

(E) *In vitro* translocation assay with control or GST-TMED10 liposomes.

(F) TMED10 proteoliposomes and TMED10-HSP90B1 proteoliposomes (HSP90B1 incorporated in the lumen) were generated. *In vitro* mL-1 β translocation assay was performed with these proteoliposomes in the presence and absence of HSP90A and ATP as indicated in the figure.

(G) *In vitro* mL-1 β translocation assay using TMED10 variant proteoliposomes, HSP90s, and ATP.

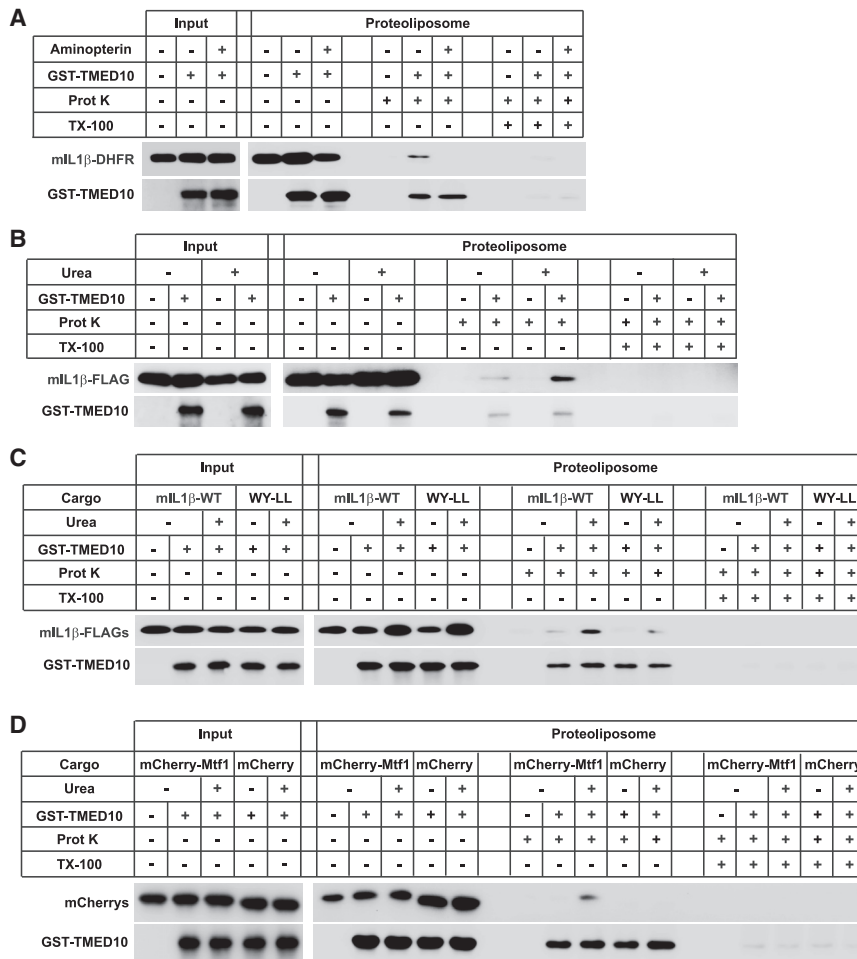


Figure 5. Protein Unfolding Regulates TMED10-Mediated Entry of mIL-1 β into the Vesicle

(A) *In vitro* membrane translocation of mIL-1 β -DHFR with control or GST-TMED10 proteoliposomes in the absence or presence of aminopterin. (B) *In vitro* membrane translocation of native mIL-1 β or mIL-1 β pre-unfolded with 6 M urea. (C) *In vitro* membrane translocation of native or urea pre-unfolded WT or WY-LL mutated mIL-1 β . (D) *In vitro* membrane translocation of native or urea pre-unfolded mCherry or mCherry with mIL-1 β motif-1 (mCherry-Mtf1).

To further examine the role of cargo unfolding, we employed a cargo pre-unfolding assay (Bauer et al., 2014). We incubated mIL-1 β with 6 M Urea to denature the cargo, making it in an unfolded state. We compared the TMED10-dependent translocation between native and pre-unfolded cargoes. In line with the DHFR-aminopterin assay, cargo pre-unfolding enhanced membrane entry of mIL-1 β (Figure 5B), indicating a preference for unfolded cargoes for TMED10-mediated translocation. Mutation of the motif-1 drastically compromised the translocation of both native and pre-folded mIL-1 β (Figures 5C and S2 [protein gel]). On the contrary, appending motif-1 to mCherry (an inert cargo for UPS as shown in Figure 3) rendered its translocation into the liposomes that was dependent on TMED10 and pre-unfolding (Figures 5D and S2 [protein gel]). Therefore, the data indicate that cargo unfolding and TMED10 interaction via motif-1 work together to facilitate the efficiency of cargo translocation.

TMED10 Promotes the Leaderless Cargo Entry into the ERGIC

To identify the membrane compartment the leaderless cargoes enter during TMED10-mediated UPS, we performed immunofluorescence. Consistent with previous results, TMED10 co-local-

ized with an ERGIC marker ERGIC53 (Jenne et al., 2002) in macrophage and non-macrophage cells (Figures 6A and S6A). A condition that triggers IL-1 β secretion leads to the co-localization of IL-1 β with the TMED10 compartment on the ERGIC (Figures 6B and 6C). In non-macrophage cells, the expressed mIL-1 β also co-localized with TMED10 (Figure S6B). In addition, the TMED10-colocalized mIL-1 β was not detected without Triton X-100 permeabilization of the ERGIC membrane suggesting mIL-1 β localizes inside the TMED10 compartment (Figures S6B and S6C). Immuno-electron microscopy confirmed the coexistence of TMED10 and mIL-1 β in a vesicular-tubular compartment (VTC) resembling the ERGIC (Figures S6D and S6E). Besides IL-1 β , we also observed the co-

localization of other leaderless cargoes with TMED10, including mIL-1 α , mIL-36 α , mIL-36RA, mIL-37, mIL-38, and HSPB5, suggesting that these cargoes also entered into the TMED10-positive compartment (Figure S6F).

To validate if the cargoes reside in the same vesicle with TMED10, we performed a fluorescence complementation assay in which we co-expressed pIL-1 β -GFP11 with TMED10 containing a luminal GFP(1-10) tag (GFP(1-10)-TMED10 (Figures 6D and 6E) (Kamiyama et al., 2016). A more than 2-fold increase of GFP level was observed under conditions stimulating IL-1 β secretion in THP-1 (Figures 6F and 6G), which supports the notion that mIL-1 β enters into the same vesicles with TMED10. An increase of fluorescence complementation was also observed in non-macrophage cells when mIL-1 β was produced by co-expressing pIL-1 β and pro-caspase-1, or mIL-1 β was directly expressed in a similar level (Figure 6H-J), indicating that the generation of mIL-1 β per se is the trigger to enter the ERGIC. The fluorescence complementation is TMED10 specific because mIL-1 β -GFP11 failed to generate GFP signal with another GFP(1-10)-tagged ERGIC protein LMAN2 (Figures S6G and S6H). Together, the data indicate that TMED10 directly facilitates the entry of leaderless cargoes into a sub-region of the ERGIC where TMED10 is enriched.

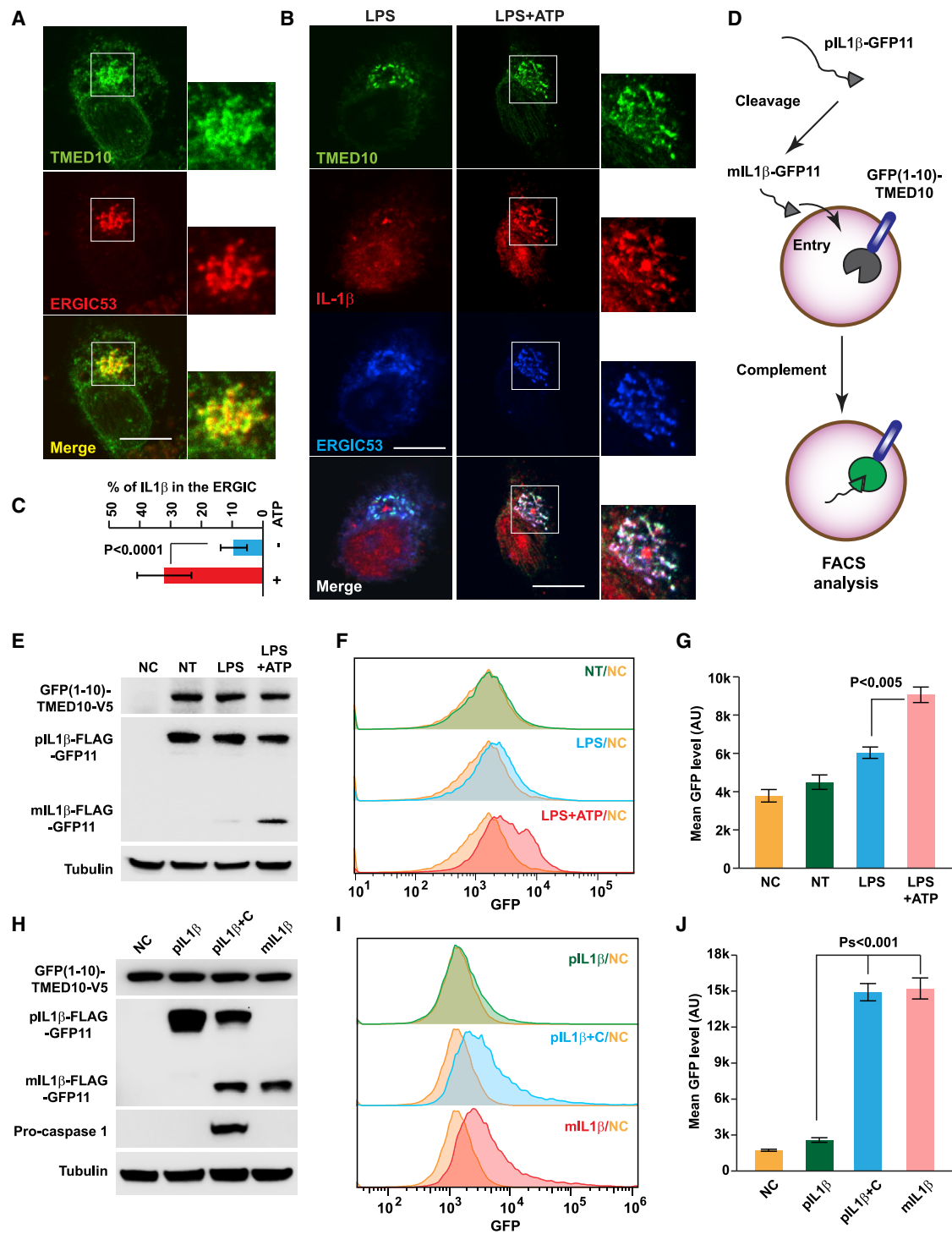


Figure 6. mIL-1β Enters into the ERGIC Positive for TMED10

(A) Immunofluorescence of THP-1 expressing TMED10-GFP with anti-ERGIC53 antibody. Scale bar, 5 μm.

(B) THP-1 expressing TMED10-GFP were primed with LPS and treated without or with ATP. Immunofluorescence was performed with anti-IL-1β and anti-ERGIC53 antibody. Scale bar, 5 μm.

(C) Quantification of the percentage of IL-1β signal in TMED10-ERGIC-positive compartment (mean ± SD). p values are indicated (two-tailed t test, n = 6).

(D) Diagram of the GFP complementation assay.

(E–G) THP-1 expressing GFP(1–10)-TMED10 and IL-1β-GFP11 were untreated (NT) or primed with LPS followed without (LPS) or with (LPS+ATP) ATP stimulation. Fluorescence-activated cell sorting (FACS) analysis was performed to determine the complemented GFP signal with cells that did not have GFP(1–10)-TMED10

(legend continued on next page)

Cargo Regulates the Oligomerization of TMED10

TMED10 is a single transmembrane protein. It is probable that TMED10 oligomerizes to form a protein channel. In colP, TMED10 associates with itself independent of a reported binding partner TMED9 (Figure S7A), and the self-association is direct (Figure S7B). In THP-1 cells, TMED10 forms high molecular weight complexes, likely to be TMED10 oligomers, in response to a condition that stimulates mL-1 β production and secretion (Figure 7A). To determine the fate of TMED10 oligomers after secretion, we induced mL-1 β secretion after which we inhibited caspase-1 to turn off secretion. We analyzed TMED10 oligomer and monomer using the crosslink assay (Figure 7B). The TMED10 oligomer gradually decreased after secretion with a corresponding increase of monomer that was not affected by proteasome inhibition (Figure 7B), indicating that TMED10 oligomer turned into monomer instead of staying oligomeric or being degraded by the proteasome after secretion.

Regarding the induction of TMED10 oligomers, it is possible that the production of a secretion-competent cargo (e.g., the generation of mL-1 β upon LPS and ATP treatment) may promote the formation of TMED10 oligomers. To test this possibility, we expressed TMED10 in the absence and presence of secretion-competent cargoes. Indeed, the presence of mL-1 β , as well as another two cargoes (mL-1 α and HSPB5), induced the high molecular weight complex formation of TMED10 (Figures 7C, S7C, and S7D), which correlated with the increase of TMED10 self-association (Figure S7E), suggesting a cargo-induced TMED10 oligomerization. We also observed a basal level of TMED10 oligomerization/self-association likely to be induced by endogenous cargoes or for other purposes (Figures 7C and S7C–S7E). The stimulatory effect of mL-1 β on oligomerization and self-association was abolished in the TMED10 Δ CT mutant that still localized to the ERGIC (Figures 7C, S7E, and S7F), suggesting that the binding of cargo to CT is required to enhance oligomerization. Consistently, the motif-1-containing mCherry that associates with TMED10 (Figure 3M) promoted TMED10 oligomerization whereas mCherry alone did not (Figure 7D).

Deletion of the GOLD domain abolished TMED10 self-association and oligomerization on the membrane (Figures S2 [protein gel] and S7G–S7J). The dimer of TMED10 Δ GD is likely a result of GST dimerization (Figures S7I and S7J). As indicated above, the GOLD domain truncation lost the ability to mediate cargo entry into the vesicle and secretion indicating the importance of oligomerization in TMED10-mediated cargo translocation (Figures 2 and 4). A requirement of the GOLD domain for TMED10 oligomerization was also reported before (Nagae et al., 2016).

DISCUSSION

How leaderless cargoes enter into the vesicle carrier in UPS has been a major question in the field. In this study, we found a

protein translocation pathway providing an implication to answer this question. Based on our data, we propose a model for the translocation process. When a secretion-competent UPS cargo (e.g., the mature form of IL-1 family members) is produced, it binds to the cytosolic HSP90A that may facilitate the unfolding of the cargo. The cargo then interacts with TMED10 on the ERGIC that induces its oligomerization to form a protein channel. With the aid of HSP90B1, the TMED10 channel translocates the cargo into the lumen of the ERGIC. Via this way, the leaderless cargoes enter into the vesicle carrier ready to be delivered out of the cell (Figure 7E). We tentatively name the pathway the TMED10-channeled UPS (THU).

The two protein translocation pathways, SEC61-mediated translocation and THU, may act in parallel to handle conventional and part of unconventional secretion. In conventional secretion, signal peptide-containing cargoes are recognized by the SRP, which directs them, together with the translation complex, to the translocon SEC61 on the ER (Rapoport et al., 2017; Shan and Walter, 2005; Voorhees and Hegde, 2016). Activated by the signal peptide and auxiliary components, the translocon is opened and the cargoes are translocated into the ER with the help of a luminal chaperone BIP co-translationally (Rapoport et al., 2017). In THU, leaderless cargoes bind to HSP90A that likely recognizes and unfolds the cargoes. Once unfolded, the cargoes may expose a signal motif (possibly motif-1) (Figure 3) that promotes the assembly of TMED10 channel (Figure 7E) and then activates translocation post-translationally. Similar to the role of BIP, the luminal chaperone HSP90B1 may act as a molecular ratchet to facilitate translocation. It is not clear whether other auxiliary components equivalent to that of the SEC61 translocon (e.g., SEC62, SEC63, or TRAP) exist to aid the TMED10 channel. (Fons et al., 2003; Lakkaraju et al., 2012; Lang et al., 2012, 2017; Sommer et al., 2013). The protein structure and dynamic regulation of the TMED10 channel are unknown too. Comprehensive structural investigation, proteomic analysis, and a cell-free reconstitution using the native membrane are necessary to further dissect THU in the near future.

The mechanism of THU is similar to another translocation process, the chaperone-mediated autophagy (CMA), in which cytosolic substrates are translocated into the lysosome for degradation through a cytosolic chaperone Hsc70, a luminal chaperone lysosomal Hsc70 and a single-transmembrane transporter LAMP2A, in which protein unfolding is required (Bandyopadhyay et al., 2008; Chiang et al., 1989; Cuervo and Dice, 1996; Kaushik and Cuervo, 2018; Salvador et al., 2000). Similar to THU, the cargoes trigger LAMP2A oligomerization that likely activates the transporter activity. An important feature of CMA is a KFERQ motif in the cytosolic cargo that is recognized by Hsc70 (Dice, 1990; Kaushik and Cuervo, 2018). Similarly, KFERQ-like motifs in mL-1 β responsible for binding the cytosolic HSP90 have

or IL-1 β -GFP11 expression as a negative control (NC). (E) Immunoblot showing the expression and processing of GFP(1–10)-TMED10 and IL-1 β -GFP11. (F) Histogram of GFP signal. (G) Quantification of GFP signal (mean \pm SD). p values are indicated (two-tailed t test, n = 3). (H–J) HEK293T was co-expressed GFP(1–10)-TMED10 with control (NC), pro-IL-1 β -FLAG-GFP11 alone (pIL-1 β), pro-IL-1 β -FLAG-GFP11 and pro-caspase 1 (pIL-1 β +C), or mL-1 β -FLAG-GFP11 (mL-1 β). FACS analysis was performed to determine the complemented GFP signal. (H) Immunoblot showing the expression and processing of IL-1 β -FLAG-GFP11 and other indicated proteins. (I) Histogram of GFP signal. (J) Quantification of GFP signal (mean \pm SD). p values are indicated (two-tailed t test, n = 3).

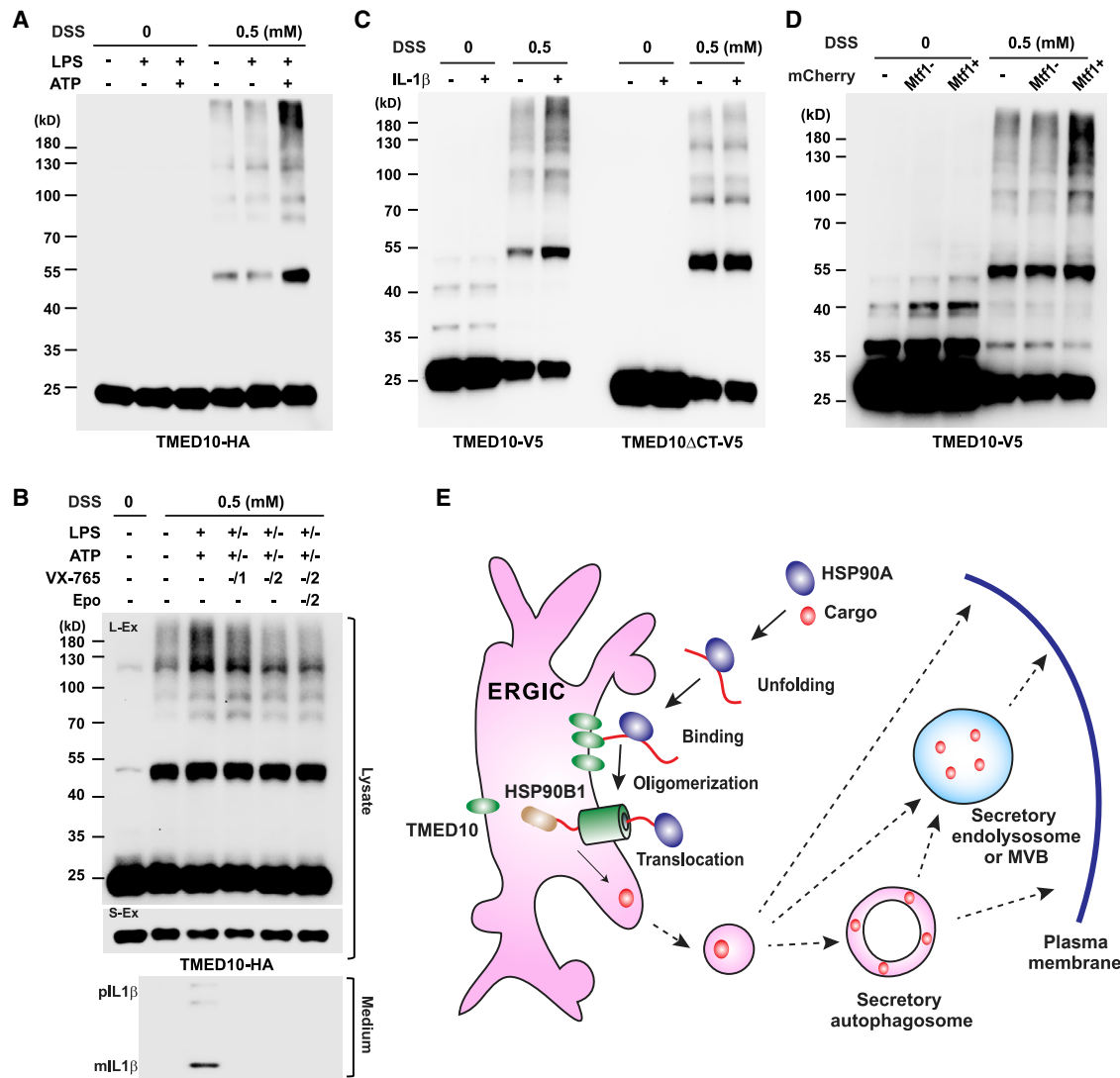


Figure 7. TMED10 Forms an Oligomer

(A) A crosslink assay performed in TMED10-HA-expressing THP-1 that was untreated or primed with LPS followed without or with ATP stimulation. (B) Disassembly of TMED10 oligomer after cargo secretion. THP-1 was untreated (lanes 1 and 2), primed with LPS followed with ATP stimulation (lane 3), or treated with LPS and ATP after which LPS and ATP was removed and replaced with medium containing 10 μ M VX-765 for 1 h (lane 4), 2 h (lane 5), or 2 h with 10 μ M epoxomicin (lane 6). Crosslink was formed on the cells to determine TMED10 oligomerization and medium was collected to analyze IL-1 β secretion. (C) A crosslink assay performed using TMED10-KO HEK293T expressing TMED10-V5 in the absence or presence of mL-1 β expression or TMED10(Δ CT)-V5 in the absence or presence of mL-1 β expression. (D) A crosslink assay performed using HEK293T expressing TMED10-V5 in the absence or presence of mCherry without or with motif-1 expression. (E) A model for TMED10-channelled UPS (THU).

been indicated in our previous study (Zhang et al., 2015). In addition, another motif (motif-1 in this study) may also determine the fate of a leaderless cargo that undergoes THU through interacting with the CT of TMED10. Although pending for further validation, it is possible that both types of selection motifs lead the cargo through the translocation process during THU. Recently, another motif, a di-acidic motif, was shown to be essential for the secretion of UPS cargoes SOD1 and Acb1 (Cruz-Garcia et al., 2017). It is not clear how this motif is recognized by the UPS machinery.

Our work indicates an activation-on-demand way of regulation in which the production of secretion-competent cargoes alone is sufficient to induce the assembly of the protein channel and activate THU. The activation-on-demand mechanism couples well with the situations when massive cargoes are produced and processed for secretion in response to certain stimuli (e.g., the massive production and maturation of an IL-1 family cytokine) (Mantovani et al., 2019). Nonetheless, our data also indicate that THU regulates the release of cargoes that may not be massively generated at once. How is THU regulated in this

case? It has been shown that stress conditions, such as starvation and oxidative stress, activates CMA via regulating the level of LAMP2A or its oligomerization (Kaushik and Cuervo, 2018). Similarly, mounting evidence indicates that the multiple types of UPS are also stimulated by stress conditions, such as starvation, ER stress, or reactive oxygen species generation (Carta et al., 2011; Chiritoiu et al., 2019; Rabouille, 2017; Sitia and Rubartelli, 2018; Tassi et al., 2010). Considering the similarity, THU is possibly regulated by stress stimuli that, together with the activation-on-demand way, makes THU able to accommodate the secretion of multiple UPS cargoes under diverse situations.

Our data imply that a sub-region of the ERGIC positive for TMED10 serves as a membrane carrier for the UPS cargos delivery in THU. In addition, secretory lysosomes, secretory autophagosomes, and multivesicular bodies (MVBs) have been shown to mediate UPS (Dimou and Nickel, 2018; Rabouille, 2017; Zhang and Schekman, 2013). It is likely that THU may cooperate with the auto/endolysosomal compartments (Figure 7E). One implication comes from our recent work indicating that the ERGIC delivers membranes to the autophagosome through a non-classical type of COPII vesicle, the ERGIC-COPII (Ge et al., 2013, 2014, 2017). Considering secretory autophagy has been proposed to regulate UPS, it is enticing to speculate that THU may cooperate with ERGIC autophagosomal membrane generation for transport of UPS cargoes (Figure 7E). It has been shown that degradative autophagosomes fuse with the endosome and lysosome to complete autophagy (Lamb et al., 2013; Mizushima, 2018; Nakamura and Yoshimori, 2017). Likewise, the secretory autophagosome may later communicate with secretory lysosomes or MVBs to achieve secretion. One piece of evidence supporting the scenario is that SEC22B, an ERGIC-enriched SNARE, cooperates with TRIM16 to regulate trafficking of IL-1 β into the secretory autophagosome (Kimura et al., 2017). Another piece of evidence is the study of the Golgi-localized protein GRASP that has been shown to regulate multiple types of UPS including type III and type VI UPS (Gee et al., 2011; Giuliani et al., 2011; Kinseth et al., 2007; Schotman et al., 2008). In yeast, the GRASP homolog Grh1 organizes the formation of a multivesicular/multilamellar compartment called CUPS. The CUPS localizes adjacent to the ER exit sites (a yeast partial equivalent of the ERGIC) and contains membranes of early Golgi, endosome, and autophagosome (Cruz-Garcia et al., 2014; Curwin et al., 2016; Dupont et al., 2011; Duran et al., 2010). In addition, GRASP controlled the IRE1 α ER-stress pathway and therefore IL-1 β secretion in macrophage (Chiritoiu et al., 2019). It is likely that GRASP may enhance the cooperation of the ERES/ERGIC and auto/endolysosome-related compartments by spatially gathering them together, in which ER stress might be involved.

The coordinated action of the ERGIC and auto/endolysosomal compartments does not rule out the possibility that they function independently. In this case, it is necessary for leaderless cargoes to enter each membrane compartment. Indeed, both the auto/endolysosomal compartments and the ERGIC may possess the ability to incorporate cargoes: autophagosomes and MVBs engulf cytosolic cargoes directly (Clague and Urbé, 2008; Mizushima, 2018). TMED10 could be a protein channel for cargo translocation into the ERGIC. Although a lysosomal transporter for UPS is pending for discovery, the CMA transporter LAMP2A

may be a candidate because it was shown that IL-1 β enters the LAMP2A-positive lysosome (Semino et al., 2018). In addition, a new UPS pathway called misfolding-associated protein secretion (MAPS) was identified in which misfolded proteins are released through encapsulation into late endosomes (Lee et al., 2016b). These studies all support the possibility that the ERGIC, autophagosome, and endolysosome are able to incorporate UPS cargoes.

In the current work, we identified TMED10 as a protein channel that regulates the secretion of a broad spectrum of UPS cargoes, including inflammatory factors (IL-1 family members and galectin 1, 3) and chaperones (HSPB5), which implies that THU may have a role in inflammation as well as multiple biological processes or pathological settings. Indeed, we found an involvement of TMED10 in regulating inflammation in a CLP-induced septic shock model (Figure 1). Others have reported a role of TMED10 in regulating neuro-inflammation in a brain-specific TMED10 transgenic mouse (Gong et al., 2011). Further, multiple studies indicated the association of altered TMED10 level with pathological conditions, including neurodegeneration and cancer (Chen et al., 2006; Nakano et al., 2017; Shin et al., 2019; Vetrivel et al., 2008; Xu et al., 2015; Zhang et al., 2018a, 2019). Although multiple roles of TMED10 in physiology and diseases have been indicated, the contribution of THU needs further clarification, considering other functions of TMED10 have also been indicated, such as regulating GPI-anchored protein transport (Fujita et al., 2011) and maintaining the ERGIC/Golgi structure (Denzel et al., 2000).

STAR★METHODS

Detailed methods are provided in the online version of this paper and include the following:

- KEY RESOURCES TABLE
- LEAD CONTACT AND MATERIALS AVAILABILITY
- EXPERIMENTAL MODEL AND SUBJECT DETAILS
 - Cells
 - *In vitro* reconstitution
 - Mice
- METHOD DETAILS
 - Plasmids and siRNA oligos
 - Reagents and antibodies
 - Transfection and secretion determination
 - Lentiviral transduction and generation of CRISPR KO cells
 - *In vitro* translocation assay
 - Proteinase K protection assay
 - Crosslink assays, immunoprecipitation, GST pull-down and immunoblot
 - Immunofluorescence, Duolink PLA and fluorescence complementation
 - Cryosectioning, immunolabeling and electron microscopy
 - Analysis of Serum IL-1 β and gene expression level
 - All-atom (AA) molecular dynamics (MD) simulations
- QUANTIFICATION AND STATISTICAL ANALYSIS
- DATA AND CODE AVAILABILITY
- ADDITIONAL RESOURCES

SUPPLEMENTAL INFORMATION

Supplemental Information can be found online at <https://doi.org/10.1016/j.cell.2020.03.031>.

ACKNOWLEDGMENTS

L.G. and M.Z. are deeply grateful to Dr. Randy Schekman for post-doctoral training at UC Berkeley and helpful suggestions on the current work. We thank Dr. Xinquan Wang, Dr. Xiaoyu Hu, Dr. Xu Tan, Dr. Yu Rao, Dr. Gong Cheng, Dr. Wanli Liu, Dr. Peng Jiang (Tsinghua University, China), Dr. Feng Shao (National Institute of Biological Sciences, China), Dr. Herbert Virgin (Vir Biotechnology), Dr. Walter Nickel (Heidelberg University, Germany), Dr. Sunao Takeshita (National Center for Geriatrics and Gerontology, Japan), and Dr. Russell Vance (UC Berkeley) for reagents. We thank Dr. Li Yu, Dr. Hongwei Wang, Dr. Ye-Guang Chen (Tsinghua University, China), Dr. Hongyan Wang (Institute of Biochemistry and Cell Biology, CAS, China), Dr. Long Li (Peking University), Dr. Bao-Liang Song (Wuhan University, China), Dr. Vivek Malhotra (CRG, Spain), Dr. Ramanuj Hegde (MRC, UK), and Dr. Catherine Rabouille (Hubrecht Institute, Netherlands) for helpful suggestions on the study. The work is funded by National Natural Science Foundation of China (91854114), National Key R&D Program of China (2019YFA0508602), National Natural Science Foundation of China (31872832, 31872826, and 31741082), State Key Laboratory of Membrane Biology (No. 2020KF09), Tsinghua Independent Research Program (2019Z06QCX02), Tsinghua-Peking Center for Life Sciences, and Thousand Young Talents Program.

AUTHOR CONTRIBUTIONS

M.Z., L.L., and L.G. performed experiments, analyzed data, and wrote the manuscript. X. Lin, Y.W., Y.L., Q.G., S.L., D.Z., X. Lv, Y.S., X.T., and L.Z. collected the data.

DECLARATION OF INTERESTS

The authors declare no competing interests.

Received: October 30, 2019

Revised: January 22, 2020

Accepted: March 11, 2020

Published: April 8, 2020

REFERENCES

Albus, C., Bjarnson-Wehrens, B., Gysan, D.B., Herold, G., Schneider, C.A., zu Eulenburg, C., and Predel, H.G.; PräFord-Studiengruppe (2012). [The effects of multimodal intervention for the primary prevention of cardiovascular diseases on depression, anxiety, and Type-D pattern: initial results of the randomized controlled PreFord trial]. *Herz* 37, 59–62.

Andrei, C., Dazzi, C., Lotti, L., Torrisi, M.R., Chimini, G., and Rubartelli, A. (1999). The secretory route of the leaderless protein interleukin 1beta involves exocytosis of endolysosome-related vesicles. *Mol. Biol. Cell* 10, 1463–1475.

Backhaus, R., Zehe, C., Wegehingel, S., Kehlenbach, A., Schwappach, B., and Nickel, W. (2004). Unconventional protein secretion: membrane translocation of FGF-2 does not require protein unfolding. *J. Cell Sci.* 117, 1727–1736.

Bailey, T.L., and Elkan, C. (1994). Fitting a mixture model by expectation maximization to discover motifs in biopolymers. *Proc. Int. Conf. Intell. Syst. Mol. Biol.* 2, 28–36.

Bandyopadhyay, U., Kaushik, S., Varticovski, L., and Cuervo, A.M. (2008). The chaperone-mediated autophagy receptor organizes in dynamic protein complexes at the lysosomal membrane. *Mol. Cell. Biol.* 28, 5747–5763.

Bauer, B.W., Shemesh, T., Chen, Y., and Rapoport, T.A. (2014). A “push and slide” mechanism allows sequence-insensitive translocation of secretory proteins by the SecA ATPase. *Cell* 157, 1416–1429.

Carta, S., Tassi, S., Pettinati, I., Delfino, L., Dinarello, C.A., and Rubartelli, A. (2011). The rate of interleukin-1beta secretion in different myeloid cells varies with the extent of redox response to Toll-like receptor triggering. *J. Biol. Chem.* 286, 27069–27080.

Chauhan, V.S., Nelson, D.A., Marriott, I., and Bost, K.L. (2013). Alpha beta-crystallin expression and presentation following infection with murine gamma-herpesvirus 68. *Autoimmunity* 46, 399–408.

Chen, F., Hasegawa, H., Schmitt-Ulms, G., Kawarai, T., Bohm, C., Katayama, T., Gu, Y., Sanjo, N., Glista, M., Rogava, E., et al. (2006). TMP21 is a presenilin complex component that modulates gamma-secretase but not epsilon-secretase activity. *Nature* 440, 1208–1212.

Chiang, H.L., Terlecky, S.R., Plant, C.P., and Dice, J.F. (1989). A role for a 70-kilodalton heat shock protein in lysosomal degradation of intracellular proteins. *Science* 246, 382–385.

Chiritoiu, M., Brouwers, N., Turacchio, G., Pirozzi, M., and Malhotra, V. (2019). GRASP55 and UPR Control Interleukin-1beta Aggregation and Secretion. *Dev. Cell* 49, 145–155.

Clague, M.J., and Urbé, S. (2008). Multivesicular bodies. *Curr. Biol.* 18, R402–R404.

Claude-Taupin, A., Jia, J., Mudd, M., and Deretic, V. (2017). Autophagy's secret life: secretion instead of degradation. *Essays Biochem.* 61, 637–647.

Claude-Taupin, A., Bissa, B., Jia, J., Gu, Y., and Deretic, V. (2018). Role of autophagy in IL-1 β export and release from cells. *Semin. Cell Dev. Biol.* 83, 36–41.

Cruz-Garcia, D., Curwin, A.J., Popoff, J.F., Bruns, C., Duran, J.M., and Malhotra, V. (2014). Remodeling of secretory compartments creates CUPS during nutrient starvation. *J. Cell Biol.* 207, 695–703.

Cruz-Garcia, D., Brouwers, N., Duran, J.M., Mora, G., Curwin, A.J., and Malhotra, V. (2017). A diacidic motif determines unconventional secretion of wild-type and ALS-linked mutant SOD1. *J. Cell Biol.* 216, 2691–2700.

Cuervo, A.M., and Dice, J.F. (1996). A receptor for the selective uptake and degradation of proteins by lysosomes. *Science* 273, 501–503.

Curwin, A.J., Brouwers, N., Alonso Y Adell, M., Teis, D., Turacchio, G., Parashuraman, S., Ronchi, P., and Malhotra, V. (2016). ESCRT-III drives the final stages of CUPS maturation for unconventional protein secretion. *eLife* 5, e16299.

Denzel, A., Otto, F., Girod, A., Pepperkok, R., Watson, R., Rosewell, I., Bergeron, J.J., Solari, R.C., and Owen, M.J. (2000). The p24 family member p23 is required for early embryonic development. *Curr. Biol.* 10, 55–58.

Dice, J.F. (1990). Peptide sequences that target cytosolic proteins for lysosomal proteolysis. *Trends Biochem. Sci.* 15, 305–309.

Dimou, E., and Nickel, W. (2018). Unconventional mechanisms of eukaryotic protein secretion. *Curr. Biol.* 28, R406–R410.

Dinarello, C.A. (2018). Overview of the IL-1 family in innate inflammation and acquired immunity. *Immunol. Rev.* 281, 8–27.

Dupont, N., Jiang, S., Pilli, M., Ornatowski, W., Bhattacharya, D., and Deretic, V. (2011). Autophagy-based unconventional secretion of α -synuclein through exophagy by impairing autophagosome-lysosome fusion. *J. Biol. Chem.* 288, 17313–17335.

Duran, J.M., Anjard, C., Stefan, C., Loomis, W.F., and Malhotra, V. (2010). Unconventional secretion of Acb1 is mediated by autophagosomes. *J. Cell Biol.* 188, 527–536.

Ejlerskov, P., Rasmussen, I., Nielsen, T.T., Bergström, A.L., Tohyama, Y., Jensen, P.H., and Vilhardt, F. (2013). Tubulin polymerization-promoting protein (TPPP/p25a) promotes unconventional secretion of α -synuclein through exophagy by impairing autophagosome-lysosome fusion. *J. Biol. Chem.* 288, 17313–17335.

Evavold, C.L., Ruan, J., Tan, Y., Xia, S., Wu, H., and Kagan, J.C. (2018). The Pore-Forming Protein Gasdermin D Regulates Interleukin-1 Secretion from Living Macrophages. *Immunity* 48, 35–44.

Fons, R.D., Bogert, B.A., and Hegde, R.S. (2003). Substrate-specific function of the translocon-associated protein complex during translocation across the ER membrane. *J. Cell Biol.* 160, 529–539.

- Fujita, M., Watanabe, R., Jaensch, N., Romanova-Michaelides, M., Satoh, T., Kato, M., Riezman, H., Yamaguchi, Y., Maeda, Y., and Kinoshita, T. (2011). Sorting of GPI-anchored proteins into ER exit sites by p24 proteins is dependent on remodeled GPI. *J. Cell Biol.* *194*, 61–75.
- Füllekrug, J., Suganuma, T., Tang, B.L., Hong, W., Storrie, B., and Nilsson, T. (1999). Localization and recycling of gp27 (hp24gamma3): complex formation with other p24 family members. *Mol. Biol. Cell* *10*, 1939–1955.
- Gardella, S., Andrei, C., Ferrera, D., Lotti, L.V., Torrisi, M.R., Bianchi, M.E., and Rubartelli, A. (2002). The nuclear protein HMGB1 is secreted by monocytes via a non-classical, vesicle-mediated secretory pathway. *EMBO Rep.* *3*, 995–1001.
- Ge, L., Wang, J., Qi, W., Miao, H.H., Cao, J., Qu, Y.X., Li, B.L., and Song, B.L. (2008). The cholesterol absorption inhibitor ezetimibe acts by blocking the sterol-induced internalization of NPC1L1. *Cell Metab.* *7*, 508–519.
- Ge, L., Qi, W., Wang, L.J., Miao, H.H., Qu, Y.X., Li, B.L., and Song, B.L. (2011). Flotillins play an essential role in Niemann-Pick C1-like 1-mediated cholesterol uptake. *Proc. Natl. Acad. Sci. USA* *108*, 551–556.
- Ge, L., Melville, D., Zhang, M., and Schekman, R. (2013). The ER-Golgi intermediate compartment is a key membrane source for the LC3 lipidation step of autophagosome biogenesis. *eLife* *2*, e00947.
- Ge, L., Zhang, M., and Schekman, R. (2014). Phosphatidylinositol 3-kinase and COPII generate LC3 lipidation vesicles from the ER-Golgi intermediate compartment. *eLife* *3*, e04135.
- Ge, L., Zhang, M., Kenny, S.J., Liu, D., Maeda, M., Saito, K., Mathur, A., Xu, K., and Schekman, R. (2017). Remodeling of ER-exit sites initiates a membrane supply pathway for autophagosome biogenesis. *EMBO Rep.* *18*, 1586–1603.
- Gee, H.Y., Noh, S.H., Tang, B.L., Kim, K.H., and Lee, M.G. (2011). Rescue of Δ F508-CFTR trafficking via a GRASP-dependent unconventional secretion pathway. *Cell* *146*, 746–760.
- Giuliani, F., Grieve, A., and Rabouille, C. (2011). Unconventional secretion: a stress on GRASP. *Curr. Opin. Cell Biol.* *23*, 498–504.
- Gong, P., Roseman, J., Fernandez, C.G., Vetrivel, K.S., Bindokas, V.P., Zitzow, L.A., Kar, S., Parent, A.T., and Thinakaran, G. (2011). Transgenic neuronal overexpression reveals that stringently regulated p23 expression is critical for coordinated movement in mice. *Mol. Neurodegener.* *6*, 87.
- Guna, A., Volkmar, N., Christianson, J.C., and Hegde, R.S. (2018). The ER membrane protein complex is a transmembrane domain insertase. *Science* *359*, 470–473.
- He, W.T., Wan, H., Hu, L., Chen, P., Wang, X., Huang, Z., Yang, Z.H., Zhong, C.Q., and Han, J. (2015). Gasdermin D is an executor of pyroptosis and required for interleukin-1 β secretion. *Cell Res.* *25*, 1285–1298.
- Huang, J., Rauscher, S., Nawrocki, G., Ran, T., Feig, M., de Groot, B.L., Grubmüller, H., and MacKerell, A.D., Jr. (2017). CHARMM36m: an improved force field for folded and intrinsically disordered proteins. *Nat. Methods* *14*, 71–73.
- Jenne, N., Frey, K., Brugger, B., and Wieland, F.T. (2002). Oligomeric state and stoichiometry of p24 proteins in the early secretory pathway. *J. Biol. Chem.* *277*, 46504–46511.
- Ji, L., Zhao, X., Zhang, B., Kang, L., Song, W., Zhao, B., Xie, W., Chen, L., and Hu, X. (2019). Slc6a8-Mediated Creatine Uptake and Accumulation Reprogram Macrophage Polarization via Regulating Cytokine Responses. *Immunity* *51*, 272–284.
- Kamiyama, D., Sekine, S., Barsi-Rhyne, B., Hu, J., Chen, B., Gilbert, L.A., Ishikawa, H., Leonetti, M.D., Marshall, W.F., Weissman, J.S., and Huang, B. (2016). Versatile protein tagging in cells with split fluorescent protein. *Nat. Commun.* *7*, 11046.
- Kaushik, S., and Cuervo, A.M. (2018). The coming of age of chaperone-mediated autophagy. *Nat. Rev. Mol. Cell Biol.* *19*, 365–381.
- Kayagaki, N., Stowe, I.B., Lee, B.L., O'Rourke, K., Anderson, K., Warming, S., Cuellar, T., Haley, B., Roose-Girma, M., Phung, Q.T., et al. (2015). Caspase-11 cleaves gasdermin D for non-canonical inflammasome signalling. *Nature* *526*, 666–671.
- Kimura, T., Jia, J., Kumar, S., Choi, S.W., Gu, Y., Mudd, M., Dupont, N., Jiang, S., Peters, R., Farzam, F., et al. (2017). Dedicated SNAREs and specialized TRIM cargo receptors mediate secretory autophagy. *EMBO J.* *36*, 42–60.
- Kinseth, M.A., Anjard, C., Fuller, D., Guizzunti, G., Loomis, W.F., and Malhotra, V. (2007). The Golgi-associated protein GRASP is required for unconventional protein secretion during development. *Cell* *130*, 524–534.
- Lakkaraju, A.K., Thankappan, R., Mary, C., Garrison, J.L., Taunton, J., and Strub, K. (2012). Efficient secretion of small proteins in mammalian cells relies on Sec62-dependent posttranslational translocation. *Mol. Biol. Cell* *23*, 2712–2722.
- Lamb, C.A., Yoshimori, T., and Tooze, S.A. (2013). The autophagosome: origins unknown, biogenesis complex. *Nat. Rev. Mol. Cell Biol.* *14*, 759–774.
- Lang, S., Benedix, J., Fedeles, S.V., Schorr, S., Schirra, C., Schäuble, N., Jalal, C., Greiner, M., Hassdenteufel, S., Tatzelt, J., et al. (2012). Different effects of Sec61 α , Sec62 and Sec63 depletion on transport of polypeptides into the endoplasmic reticulum of mammalian cells. *J. Cell Sci.* *125*, 1958–1969.
- Lang, S., Pfeffer, S., Lee, P.H., Cavalié, A., Helms, V., Förster, F., and Zimmermann, R. (2017). An Update on Sec61 Channel Functions, Mechanisms, and Related Diseases. *Front. Physiol.* *8*, 887.
- Lee, J., Cheng, X., Swails, J.M., Yeom, M.S., Eastman, P.K., Lemkul, J.A., Wei, S., Buckner, J., Jeong, J.C., Qi, Y., et al. (2016a). CHARMM-GUI input generator for NAMD, GROMACS, AMBER, OpenMM, and CHARMM/OpenMM simulations using the CHARMM36 additive force field. *J. Chem. Theory Comput.* *12*, 405–413.
- Lee, J.G., Takahama, S., Zhang, G., Tomarev, S.I., and Ye, Y. (2016b). Unconventional secretion of misfolded proteins promotes adaptation to proteasome dysfunction in mammalian cells. *Nat. Cell Biol.* *18*, 765–776.
- Lock, R., Kenific, C.M., Leidal, A.M., Salas, E., and Debnath, J. (2014). Autophagy-dependent production of secreted factors facilitates oncogenic RAS-driven invasion. *Cancer Discov.* *4*, 466–479.
- Lopez-Castejon, G., Theaker, J., Pelegrin, P., Clifton, A.D., Braddock, M., and Surprenant, A. (2010). P2X(7) receptor-mediated release of cathepsins from macrophages is a cytokine-independent mechanism potentially involved in joint diseases. *J. Immunol.* *185*, 2611–2619.
- Lu, Y., Qiu, Y., Chen, P., Chang, H., Guo, L., Zhang, F., Ma, L., Zhang, C., Zheng, X., Xiao, J., et al. (2019). ER-localized Hrd1 ubiquitinates and inactivates Usp15 to promote TLR4-induced inflammation during bacterial infection. *Nat. Microbiol.* *4*, 2331–2346.
- Malhotra, V. (2013). Unconventional protein secretion: an evolving mechanism. *EMBO J.* *32*, 1660–1664.
- Mantovani, A., Dinarello, C.A., Molgora, M., and Garlanda, C. (2019). Interleukin-1 and Related Cytokines in the Regulation of Inflammation and Immunity. *Immunity* *50*, 778–795.
- Mizushima, N. (2018). A brief history of autophagy from cell biology to physiology and disease. *Nat. Cell Biol.* *20*, 521–527.
- Monteleone, M., Stanley, A.C., Chen, K.W., Brown, D.L., Bezbradica, J.S., von Pein, J.B., Holley, C.L., Boucher, D., Shakespeare, M.R., Kapetanovic, R., et al. (2018). Interleukin-1 β Maturation Triggers Its Relocation to the Plasma Membrane for Gasdermin-D-Dependent and -Independent Secretion. *Cell Rep.* *24*, 1425–1433.
- Nagae, M., Hirata, T., Morita-Matsumoto, K., Theiler, R., Fujita, M., Kinoshita, T., and Yamaguchi, Y. (2016). 3D Structure and Interaction of p24 β and p24 δ Golgi Dynamics Domains: Implication for p24 Complex Formation and Cargo Transport. *J. Mol. Biol.* *428*, 4087–4099.
- Nakamura, S., and Yoshimori, T. (2017). New insights into autophagosome-lysosome fusion. *J. Cell Sci.* *130*, 1209–1216.
- Nakano, N., Tsuchiya, Y., Kako, K., Umezaki, K., Sano, K., Ikeno, S., Otsuka, E., Shigeta, M., Nakagawa, A., Sakata, N., et al. (2017). TMED10 Protein Interferes with Transforming Growth Factor (TGF)- β Signaling by Disrupting TGF- β Receptor Complex Formation. *J. Biol. Chem.* *292*, 4099–4112.
- Nickel, W., and Rabouille, C. (2009). Mechanisms of regulated unconventional protein secretion. *Nat. Rev. Mol. Cell Biol.* *10*, 148–155.

- Pantazopoulou, A., and Glick, B.S. (2019). A Kinetic View of Membrane Traffic Pathways Can Transcend the Classical View of Golgi Compartments. *Front. Cell Dev. Biol.* *7*, 153.
- Pastor-Cantizano, N., Montesinos, J.C., Bernat-Silvestre, C., Marcote, M.J., and Aniento, F. (2016). p24 family proteins: key players in the regulation of trafficking along the secretory pathway. *Protoplasma* *253*, 967–985.
- Pierce, B.G., Hourai, Y., and Weng, Z. (2011). Accelerating protein docking in ZDOCK using an advanced 3D convolution library. *PLoS ONE* *6*, e24657.
- Popa, S.J., Stewart, S.E., and Moreau, K. (2018). Unconventional secretion of annexins and galectins. *Semin. Cell Dev. Biol.* *83*, 42–50.
- Pronk, S., Páll, S., Schulz, R., Larsson, P., Bjelkmar, P., Apostolov, R., Shirts, M.R., Smith, J.C., Kasson, P.M., van der Spoel, D., et al. (2013). GROMACS 4.5: a high-throughput and highly parallel open source molecular simulation toolkit. *Bioinformatics* *29*, 845–854.
- Qu, Y., Franchi, L., Nunez, G., and Dubyak, G.R. (2007). Nonclassical IL-1 beta secretion stimulated by P2X7 receptors is dependent on inflammasome activation and correlated with exosome release in murine macrophages. *J. Immunol.* *179*, 1913–1925.
- Rabouille, C. (2017). Pathways of Unconventional Protein Secretion. *Trends Cell Biol.* *27*, 230–240.
- Rabouille, C., Malhotra, V., and Nickel, W. (2012). Diversity in unconventional protein secretion. *J. Cell Sci.* *125*, 5251–5255.
- Rapoport, T.A., Li, L., and Park, E. (2017). Structural and Mechanistic Insights into Protein Translocation. *Annu. Rev. Cell Dev. Biol.* *33*, 369–390.
- Rubartelli, A., Cozzolino, F., Talio, M., and Sitia, R. (1990). A novel secretory pathway for interleukin-1 beta, a protein lacking a signal sequence. *EMBO J.* *9*, 1503–1510.
- Ruiz, S., Vardon-Bouines, F., Merlet-Dupuy, V., Conil, J.M., Buléon, M., Fourcade, O., Tack, I., and Minville, V. (2016). Sepsis modeling in mice: ligation length is a major severity factor in cecal ligation and puncture. *Intensive Care Med. Exp.* *4*, 22.
- Salvador, N., Aguado, C., Horst, M., and Knecht, E. (2000). Import of a cytosolic protein into lysosomes by chaperone-mediated autophagy depends on its folding state. *J. Biol. Chem.* *275*, 27447–27456.
- Schäfer, T., Zentgraf, H., Zehe, C., Brügger, B., Bernhagen, J., and Nickel, W. (2004). Unconventional secretion of fibroblast growth factor 2 is mediated by direct translocation across the plasma membrane of mammalian cells. *J. Biol. Chem.* *279*, 6244–6251.
- Schatz, G., and Dobberstein, B. (1996). Common principles of protein translocation across membranes. *Science* *271*, 1519–1526.
- Schneider, C.A., Rasband, W.S., and Eliceiri, K.W. (2012). NIH Image to ImageJ: 25 years of image analysis. *Nat. Methods* *9*, 671–675.
- Schotman, H., Karhinen, L., and Rabouille, C. (2008). dGRASP-mediated non-canonical integrin secretion is required for *Drosophila* epithelial remodeling. *Dev. Cell* *14*, 171–182.
- Semino, C., Carta, S., Gattorno, M., Sitia, R., and Rubartelli, A. (2018). Progressive waves of IL-1 β release by primary human monocytes via sequential activation of vesicular and gasdermin D-mediated secretory pathways. *Cell Death Dis.* *9*, 1088.
- Shan, S.O., and Walter, P. (2005). Co-translational protein targeting by the signal recognition particle. *FEBS Lett.* *579*, 921–926.
- Shi, J., Zhao, Y., Wang, K., Shi, X., Wang, Y., Huang, H., Zhuang, Y., Cai, T., Wang, F., and Shao, F. (2015). Cleavage of GSDMD by inflammatory caspases determines pyroptotic cell death. *Nature* *526*, 660–665.
- Shin, J.H., Park, S.J., Jo, D.S., Park, N.Y., Kim, J.B., Bae, J.E., Jo, Y.K., Hwang, J.J., Lee, J.A., Jo, D.G., et al. (2019). Down-regulated TMED10 in Alzheimer disease induces autophagy via ATG4B activation. *Autophagy* *15*, 1495–1505.
- Sitia, R., and Rubartelli, A. (2018). The unconventional secretion of IL-1 β : Handling a dangerous weapon to optimize inflammatory responses. *Semin. Cell Dev. Biol.* *83*, 12–21.
- Slot, J.W., and Geuze, H.J. (2007). Cryosectioning and immunolabeling. *Nat. Protoc.* *2*, 2480–2491.
- Sommer, N., Junne, T., Kalies, K.U., Spiess, M., and Hartmann, E. (2013). TRAP assists membrane protein topogenesis at the mammalian ER membrane. *Biochim. Biophys. Acta* *1833*, 3104–3111.
- Steringer, J.P., and Nickel, W. (2018). A direct gateway into the extracellular space: Unconventional secretion of FGF2 through self-sustained plasma membrane pores. *Semin. Cell Dev. Biol.* *83*, 3–7.
- Takeshita, S., Kaji, K., and Kudo, A. (2000). Identification and characterization of the new osteoclast progenitor with macrophage phenotypes being able to differentiate into mature osteoclasts. *J. Bone Miner. Res.* *15*, 1477–1488.
- Tassi, S., Carta, S., Delfino, L., Caorsi, R., Martini, A., Gattorno, M., and Rubartelli, A. (2010). Altered redox state of monocytes from cryopyrin-associated periodic syndromes causes accelerated IL-1 β secretion. *Proc. Natl. Acad. Sci. USA* *107*, 9789–9794.
- Verhoef, P.A., Estacion, M., Schilling, W., and Dubyak, G.R. (2003). P2X7 receptor-dependent blebbing and the activation of Rho-effector kinases, caspases, and IL-1 beta release. *J. Immunol.* *170*, 5728–5738.
- Vetrivel, K.S., Kodam, A., Gong, P., Chen, Y., Parent, A.T., Kar, S., and Thirakaran, G. (2008). Localization and regional distribution of p23/TMP21 in the brain. *Neurobiol. Dis.* *32*, 37–49.
- Villeneuve, J., Bassaganyas, L., Lepreux, S., Chiritoiu, M., Costet, P., Ripoché, J., Malhotra, V., and Schekman, R. (2018). Unconventional secretion of FABP4 by endosomes and secretory lysosomes. *J. Cell Biol.* *217*, 649–665.
- Voorhees, R.M., and Hegde, R.S. (2016). Toward a structural understanding of co-translational protein translocation. *Curr. Opin. Cell Biol.* *41*, 91–99.
- Xu, X., Gao, H., Qin, J., He, L., and Liu, W. (2015). TMP21 modulates cell growth in papillary thyroid cancer cells by inducing autophagy through activation of the AMPK/mTOR pathway. *Int. J. Clin. Exp. Pathol.* *8*, 10824–10831.
- Yang, J., Yan, R., Roy, A., Xu, D., Poisson, J., and Zhang, Y. (2015). The I-TASSER Suite: protein structure and function prediction. *Nat. Methods* *12*, 7–8.
- Zanetti, G., Pahuja, K.B., Studer, S., Shim, S., and Schekman, R. (2011). COPII and the regulation of protein sorting in mammals. *Nat. Cell Biol.* *14*, 20–28.
- Zhang, M., and Schekman, R. (2013). Cell biology. Unconventional secretion, unconventional solutions. *Science* *340*, 559–561.
- Zhang, M., Kenny, S.J., Ge, L., Xu, K., and Schekman, R. (2015). Translocation of interleukin-1 β into a vesicle intermediate in autophagy-mediated secretion. *eLife* *4*, e11205.
- Zhang, X., Wu, Y., Cai, F., Liu, S., Bromley-Brits, K., Xia, K., and Song, W. (2018a). A Novel Alzheimer-Associated SNP in Tmp21 Increases Amyloidogenesis. *Mol. Neurobiol.* *55*, 1862–1870.
- Zhang, Z., Wei, Y., Liu, B., Wu, Y., Wang, H., Xie, X., Feng, Z., Shao, G., and Xiong, Q. (2018b). Hsp90/Sec22b promotes unconventional secretion of mature-IL-1 β through an autophagosomal carrier in porcine alveolar macrophages during *Mycoplasma hypopneumoniae* infection. *Mol. Immunol.* *101*, 130–139.
- Zhang, X., Wu, Y., Cai, F., and Song, W. (2019). Regulation of global gene expression in brain by TMP21. *Mol. Brain* *12*, 39.

STAR★METHODS

KEY RESOURCES TABLE

REAGENT or RESOURCE	SOURCE	IDENTIFIER
Antibodies		
Rabbit polyclonal anti-TMED10	Proteintech	Cat# 15199-1-AP; RRID: AB_2204321
Rabbit polyclonal anti-TMED9	Proteintech	Cat# 21620-1-AP; RRID: AB_10858623
Rabbit polyclonal anti-IL-1 β	Abcam	Cat# Ab9722; RRID: AB_308765
Mouse monoclonal anti-FLAG	Sigma	Cat# F3165; RRID: AB_259529
Rabbit monoclonal anti-caspase-1	CST	Cat# 3866; RRID: AB_2069051
Rabbit monoclonal anti-HA	CST	Cat# 3724; RRID: AB_1549585
Mouse monoclonal anti-T7	Sigma	Cat# 69522; RRID: AB_11211744
Rabbit polyclonal anti-GSDMD	Dr. Feng Shao	N/A
Rabbit polyclonal anti-ERGIC53	Sigma	Cat# E1031; RRID: AB_532237
Mouse monoclonal anti-GST	CST	Cat# 2624; RRID: AB_2189875
Rabbit monoclonal anti-V5	CST	Cat# 13202; RRID: AB_2687461
Rabbit monoclonal anti-GFP (WB)	CST	Cat# 2956; RRID: AB_1196615
Rabbit polyclonal anti-GFP (EM)	Abcam	Cat# ab6556; RRID: AB_305564
Mouse monoclonal anti-HSP90A	Santa Cruz	Cat# sc-13119; RRID: AB_675659
Rabbit polyclonal anti-HSP90B1(GRP94)	Proteintech	Cat# 14700-1-AP; RRID: AB_2233347
Rabbit monoclonal anti-mCherry	CST	Cat# 43590; RRID: AB_2799246
Mouse monoclonal anti-Tubulin	Abcam	Cat# ab7291; RRID: AB_2241126
Mouse monoclonal anti-Actin	Abcam	Cat# ab8224; RRID: AB_449644
Rabbit polyclonal anti-Ribophorin1(RPN1)	Dr. Randy Schekman	N/A
Rabbit polyclonal anti-SEC22B	Dr. Randy Schekman	N/A
Mouse monoclonal anti-PDI	Enzo	Cat# ADI-SPA-891; RRID: AB_10615355
Chemicals, Peptides, and Recombinant Proteins		
DSS	Thermo Scientific	Cat# 21555
DSP	Thermo Scientific	Cat# A35393
Punicalagin	Selleck	Cat# s9131
VX-765	Selleck	Cat# S2228
Epoxomicin	Selleck	Cat# S7038
Aminopterin	Sigma	Cat# A1784
Anti-FLAG agarose	Sigma	Cat# A2220
Anti-HA agarose	Sigma	Cat# A2095
Anti-V5 agarose	Sigma	Cat# A7345
ATP	InvivoGen	Cat# tlrl-atpl
LPS	InvivoGen	Cat# tlrl-3pelps
GST-TMED10 protein	This paper	N/A
mIL-1 β -FLAG protein	This paper	N/A
Critical Commercial Assays		
Duolink PLA kit	Sigma	Cat# DUO92102
IL-1 β Mouse Uncoated ELISA Kit	Thermo Scientific	Cat# 88-7013-22
QUANTI-Blue	InvivoGen	Cat# rep-qbs
LDH Cytotoxicity Assay Kit	Thermo Scientific	Cat# 88953
Experimental Models: Cell Lines		
HEK293T Cells	Dr. Randy Schekman	N/A
U2OS Cells	Dr. Randy Schekman	N/A

(Continued on next page)

Continued

REAGENT or RESOURCE	SOURCE	IDENTIFIER
HEK-Blue IL-1 β Cells	InvivoGen	Cat# hkb-il1b
THP-1 Cells	Dr. Gong Cheng	N/A
HeLa cells and GSDMD KO HeLa cells	Dr. Feng Shao	N/A
CMG14-12 cells	Dr. Sunao Takeshita	N/A
HL-60 Cells	Dr. Yu Rao	N/A
MPDM Cells	Dr. Herbert Virgin	N/A
HEK293T-TMED10 KO cells	This paper	N/A
THP-1-TMED10 KO cells	This paper	N/A
Experimental Models: Organisms/Strains		
TMED10 fl/fl mice (C57BL/6J)	GemPharmatech Co. Ltd	N/A
Lyz2-Cre mice (C57BL/6J)	Dr. Xiaoyu Hu	N/A
Oligonucleotides		
Oligos for shRNAs, see Table S2	This paper	N/A
siRNAs for TMED10	QIAGEN	Cat# GS10972
IL6(F)-QPCR primer TGTATGAACAACGATGATGCACTT	Lu et al., 2019	N/A
IL6(R)-QPCR primer ACTCTGGCTTTGTCTTTCTTGTATCT	Lu et al., 2019	N/A
GAPDH(F)-QPCR primer GTTCTACCCCAATGTGTCC	This paper	N/A
GAPDH(R)- QPCR primer TAGCCCAAGATGCCCTTCAGT	This paper	N/A
TMED10-Flox(F)-genotyping primer AATGCCATGCCTGTAACCTGGG	GemPharmatech Co. Ltd	N/A
TMED10-Flox(R)-genotyping primer TTGTTTCTTGAGGGGCATAGCA	GemPharmatech Co. Ltd	N/A
Recombinant DNA		
pLX304-TMED10-V5	DNAsu	JF432606
pGEX4T1-TMED10	This paper	N/A
pFUGW-GFP(1-10)-TMED10-V5	This paper	N/A
pFUGW-mIL-1 β -FLAG	This paper	N/A
pFUGW-pIL-1 β -FLAG	This paper	N/A
pFUGW-mIL-1 β -FLAG-GFP11	This paper	N/A
pFUGW-pIL-1 β -FLAG-GFP11	This paper	N/A
pFUGW-mIL-1 α -FLAG	This paper	N/A
pFUGW-mIL-18-FLAG	This paper	N/A
pFUGW-mIL-33-FLAG	This paper	N/A
pFUGW-mIL-36 α -FLAG	This paper	N/A
pFUGW-mIL-36 β -FLAG	This paper	N/A
pFUGW-mIL-36 γ -FLAG	This paper	N/A
pFUGW-mIL-36RA-FLAG	This paper	N/A
pFUGW-mIL-37-FLAG	This paper	N/A
pFUGW-mIL-38-FLAG	This paper	N/A
pFUGW-HA-HSPB5	This paper	N/A
pET28a-mIL-1 β -FLAG	This paper	N/A
pET28a-mIL-18-FLAG	This paper	N/A
pET28a-mIL-36 α -FLAG	This paper	N/A
pET28a-mIL-37-FLAG	This paper	N/A
pET28a-HSP90A	This paper	N/A

(Continued on next page)

Continued

REAGENT or RESOURCE	SOURCE	IDENTIFIER
pGEX4T1-HSP90B1	This paper	N/A
Software and Algorithms		
Fiji (ImageJ)	Schneider et al., 2012	https://imagej.nih.gov/ij/
Prism 8	GraphPad	https://www.graphpad.com
Flowjo	FLOWJO	https://www.flowjo.com/
CHARMM-GUI	Lee et al., 2016a	http://www.charmm-gui.org/
GROMACS	Pronk et al., 2013	http://www.gromacs.org/

LEAD CONTACT AND MATERIALS AVAILABILITY

Further information and requests for reagents should be directed to Lead Contact, Liang Ge (liangge@mail.tsinghua.edu.cn). Plasmids, TMED10-Loxp mice, and cell lines generated in this study will be made available upon request. We may require a payment and/or a completed Materials Transfer Agreement in case there is potential for commercial application.

EXPERIMENTAL MODEL AND SUBJECT DETAILS

Cells

Cells were maintained in DMEM (HEK293T, U2OS, HeLa (GSDMD-KO HeLa were obtained from Dr. Feng Shao)) or RPMI-1640 (THP-1 (from Dr. Gong Cheng), HL-60 (from Dr. Yu Rao)) supplemented with 10% FBS at 37°C in 5% CO₂. MPDM (from Dr. Herbert Virgin) was maintained in RPMI-1640 supplemented with 10% FBS, 1% Pen-Strep-Glut (Thermo), 30 μM BME, 10% conditioned medium from CMG14-12 cells (from Dr. Sunao Takeshita) ([Takeshita et al., 2000](#)) (approximately 20 ng/ml GM-CSF) and 1 μM β-estrogen. For MPDM differentiation, β-estrogen was excluded from the culture medium. CMG14-12 was maintained in DMEM supplemented with 10% heat-inactivated FBS and G418 (400 μg/mL). For producing GM-CSF, CMG14-12 was maintained in the medium in the absence of G418 for two days at the confluency of 100%.

In vitro reconstitution

The *in vitro* reconstitution contains steps of protein purification, proteoliposome creation and *in vitro* translocation. For protein purification, BL21 *E. Coli* was transformed with plasmids encoding the proteins. Single colonies were picked and incubated at 37°C in a shaker overnight. The culture was further expanded to 50-100 mL and incubated overnight similarly after which the culture was 1:50 diluted with 0.5-1 L fresh medium followed by incubating at 37°C in a shaker for 1-2 h until the OD₆₀₀ reached to 0.6-0.8. IPTG (100 μM) was added to the culture and the protein expression was induced at 22°C for 5h with shaking. Protein purification was described in detail below. For proteoliposome creation, different kinds of TMED10 proteins (dissolved in Triton X-100) were incubated with phospholipids (dissolved in Triton X-100) extracted from HEK293T cells. Proteoliposomes were formed by gradually removing the detergent by Biobeads. For *in vitro* translocation, the purified cargo proteins were incubated with proteoliposomes with TMED10 with or without HSP90s at 30°C in the test tube for 1 h. A membrane flotation and proteinase K digestion were performed following the *in vitro* translocation (see below for details).

Mice

The mice experiments were approved by the Institutional Animal Care and Use Committees at Tsinghua University. Mice were housed in ventilated cages in a temperature and light regulated room in a SPF facility and received food and water *ad libitum*. TMED10 fl/fl mice (C57BL/6J) were created by GemPharmatech Co. Ltd, China. Mice with myeloid cell lineage-specific TMED10 deletion were generated via crossbreeding with Lyz2-Cre mice (C57BL/6J) ([Ji et al., 2019](#)), a kind gift from Dr. Xiaoyu Hu lab at Tsinghua University. The CLP experiments were performed as described previously ([Lu et al., 2019](#); [Ruiz et al., 2016](#)). In brief, 8-12 weeks' old mice, 6-10 mice per group (see detail in figure legends) with half male and female, were anesthetized and an abdominal incision was made to allow for ligation of the distal one-third of the caecum with a silk suture followed by two punctures with a 21-gauge needle. A small amount of caecal content was extruded through the puncture. After relocating the caecum to the abdomen, the incision was closed and 1 mL saline was injected intraperitoneally for resuscitation. For the mock-treated mice, the same steps, except for the puncture were performed.

METHOD DETAILS

Plasmids and siRNA oligos

The mature forms of IL-1 family members (p-IL-1 β from Russell Vance, p-IL-18 from Sinobiological, pIL-36RA, α , β , γ and 37 from Dr. Xinquan Wang, the others were amplified from cDNA) were PCR amplified from templates of pro-forms and inserted into the FUGW vector with a FLAG tag at the C terminus. Mutagenesis was formed by PCR. mL-1 β , mL-36 α , mL-37 and mL-38 were inserted into PET28a vector for protein purification. The mL-1 β -FLAG-DHFR plasmid was constructed by subcloning the DHFR from MTS-GFP-DHFR (provided Dr. Walter Nickel) into the C terminus of mL-1 β -FLAG. We also obtained α -synuclein from OriGene, Tau and Galectin-1 from Addgene, IL-6 and FGF2 from Sinobiological, TAT from Dr. Xu Tan. Galectin-3 and Annexin A1 were PCR amplified from cDNAs. The TMED10-V5 plasmid was from DNASU. The TMED10 truncations were generated by mutagenesis PCR. The TMED10 variants were also inserted into PGEX4T1 vector for protein purification. The p-caspase-1 and HSP90A plasmids were from Addgene. The HSP90B1 was PCR amplified from cDNA and inserted into plasmids for mammalian cell expression and prokaryote protein purification.

For shRNAs, pLKO.1 lentivirus vector (Addgene) was used to introduce short hairpin RNAs (shRNAs). As previously described (Zhang et al., 2015). The targeting sequences used to knock down the genes by shRNAs were shown in Table S2.

For siRNAs, an equimolar mixture of 4 different siRNAs (Flexi Tube Hs TMP21-4, Hs TMED10-1, -3 and -4; QIAGEN) was used to induce TMED10 silencing. AllStars negative siRNA (QIAGEN) was used as a control.

Reagents and antibodies

We obtained DSS and DSP from Thermo, punicalagin, VX-765 and epoxomicin from Selleck, aminopterin, proteinase K, protease inhibitor cocktail, anti-FLAG M2 agarose, anti-V5 agarose, anti-HA agarose and Duolink PLA kit from Sigma, Phenylmethylsulfonyl fluoride (PMSF) from Amresco. Mouse anti-FLAG, anti-tubulin, goat anti-IL-1 β , rabbit anti-IL-1 β , anti-RPN1, anti-SEC22B, and anti-ERGIC53 antibodies were described before (Zhang et al., 2015). We purchased mouse anti-HSP90A antibody from Santa Cruz, rabbit anti-HSP90B1, anti-TMED10 and anti-TMED9 from Proteintech, rabbit anti-Caspase-1, anti-V5, anti-HA, anti-GST, anti-GFP and anti-mCherry antibodies from CST, mouse anti-T7 antibody from Sigma. Rabbit anti-GSDMD antibody is a general gift from Dr. Feng Shao.

Transfection and secretion determination

Transfection of DNA constructs into cells was performed using PEI (Polysciences, Inc.) for HEK293T and X-tremeGENE HP (Roche) for U2OS according to the manufacture's protocols. The siRNA transfection was performed with Lipofectamine RNAiMAX (Invitrogen) according to the manufacture's protocols.

For determination of cargo secretion, cells (general cell lines) were replaced with DMEM for 1 hour or induced with 100ng/ml LPS overnight in RPMI-1640 plus 10% FBS followed by 2 mM ATP treatment for 30 min in physiological saline solution (147 mM NaCl, 10 mM HEPES pH 7.4, 13 mM glucose, 2 mM CaCl₂, 1 mM MgCl₂, 2 mM KCl) (Lopez-Castejon et al., 2010). The medium was concentrated (20-fold) by a 10 kD Amicon filter (Millipore) and cell lysate was collected. Immunoblot was performed to determine the amount of cargoes in the medium and cell. LDH assay (Thermo) and SEAP (InvivoGen) were performed according to the manufacturers' protocol.

Lentiviral transduction and generation of CRISPR KO cells

For lentiviral transduction, pLKO.1 plasmids containing the shRNA constructs (together with lentiviral packaging plasmids pMD2.G and psPAX2 (Addgene)), pLX304 plasmids containing the TMED10-V5, FUGW, or LentiCRISPRv2 (Addgene) (together with VSVG and psPAX2) were transfected into HEK293T cells to produce lentiviral particles for 60-72 h. The supernatant was collected to infect the indicated inflammatory cells.

For the generation of TMED10-KO cell lines in HEK293T, the cells were transfected with PX330 containing TMED10 targeting sequences (sgRNA sequences: TCCGGCGCGTTGAGGCCTT & TAACGAAAAGGGCCGCGCC). For the generation of THP-1 or HL-60 TMED10-KO cell lines, the cells were infected with LentiCRISPRv2 virus containing the same TMED10 targeting sequences indicated above. For the generation of GSDMD-KO THP-1, the cells were infected with LentiCRISPRv2 virus containing the GSDMD targeting sequences (sgRNA sequences: TCTCCGGACTACCCGCTCAA & CGGCCTTTGAGCGGGTAGTC). The cells were then diluted and single colonies were isolated and determined for TMED10 KO.

In vitro translocation assay

For protein purification, genes encoding IL-1s and HSP90A were inserted into the PET28a vector, and genes encoding TMED10s and HSP90B were inserted into the PGEX4T1 vector. The proteins were expressed in BL21 *E. Coli* at 22°C for 5h (note: TMED10 is not glycosylated (data not shown) and therefore we purify the protein from BL21). After expression, the bacteria were collected and digested with 0.5mg/ml lysozyme (Sigma) in lysis buffer (50mM Tris/HCl pH 8.0, 5mM EDTA, 150mM NaCl, 10% glycerol for GST protein purification, or 2x PBS, 10mM imidazole for His protein purification) plus 0.3mM DTT and protease inhibitors on ice for 0.5h. Triton X-100 was added to adjust to 0.5% final concentration. The lysates were sonicated and centrifuged at 20,000xg for 1h. The supernatants were incubated with Glutathione Agarose or Ni-NTA Agarose (Thermo) and rotated at 4°C for 2h. The agarose

was washed with 10 bed volume of wash buffer with 0.1% Tween20 and wash buffer each (PBS for GST protein purification or 2xPBS+25mM imidazole for His protein purification). For purification of TMED10s, 0.5% Triton X-100 was included in all procedures. The proteins were eluted by elution buffers (50mM Tris 8.0, 250mM KCl, 25mM glutathione for GST proteins or 2x PBS, 250mM imidazole for His proteins) and concentrated by Amicon® Ultra Filters (Merck). FPLC was performed for buffer exchange and increase of purity. The proteins were snap frozen by liquid nitrogen and stored in PBS (0.5% Triton X-100 for TMED10s) at 80°C.

Total Lipids were extracted from HEK293T cells. Each 300 μ L cell suspension was incubated with 1.2 mL chloroform/methanol solution (chloroform: methanol = 1:2) and vortexed for 30 s and shaken for 1h at 180 rpm at 37°C. Chloroform phase was collected and was evaporated by a stream of nitrogen gas over the lipid solution and further dried in 37°C incubator for 1h. Dried lipid was suspended in HEPES-KAc buffer contain 20mM HEPES (pH 7.2) and 150mM potassium acetate. The phosphatidylcholine content of lipid solution was measured and used as a standard to normalize lipid concentration. The lipid was aliquoted and stored in -80°C.

Proteoliposome reconstitution was performed according to a previous report with modifications (Guna et al., 2018). The lipids were repeatedly frozen in liquid nitrogen and thawed in 42°C water bath for 10 times. Add Triton X-100 into lipid solution to a final concentration of 0.05% and rotated in 4°C for 30min. Recombinant proteins were added into the lipid solution (400 μ L solution contain 10 μ g GST-TMED10, with or without 72 μ g HSP90B1, and 1.25 mg lipid) and incubated for another 1h with rotation. Each 400 μ L solution was incubated with 6-8mg Biobeads SM2 (Bio-rad) equilibrated with the HEPES-KAc buffer at 4°C. Beads were replaced each hour and repeated for 5 times (10 mg beads in the third time and incubated overnight). After a 1,500 xg centrifugation to remove the Biobeads, the liposome solution was repeatedly frozen in liquid nitrogen and thawed in 42°C water bath for 5 times. In order to remove the free proteins, a membrane flotation procedure was performed. For each 300 μ L solution, 300 μ L 50% OptiPrep (diluted in HEPES-KAc buffer) was added. The mixture was overlaid with 480 μ L 20% OptiPrep and 90 μ L HEPES-KAc buffer, centrifuged at 100,000 xg for 2h and the 150 μ L top fraction (which contains the proteoliposomes) was collected and diluted with 150 μ L HEPES-KAc buffer.

For the *in vitro* IL-1 β translocation, recombinant proteins (150 μ L reaction system contain 6 μ g mL-1 β , with or without 2.7 μ g HSP90A) and with or without ATP(5mM final concentration) were added to proteoliposome solution, incubated for 1h in 30°C. After then, an equal volume of 50% OptiPrep (diluted in HEPES-KAc buffer) was added followed by overlaying with 240 μ L 20% OptiPrep, 45 μ L HEPES-KAc buffer, and centrifuged at 45,000 rpm for 2h. The proteoliposomes (90 μ L fraction from the top) were aliquoted into 3 fractions. The first fraction was a control, the second and third fractions were digested by protease K (10 μ g/ml) without or with 0.5% Triton X-100 for 20 min on ice. The reactions were stopped by 1mM PMSF and incubated for 10min on ice. Then SDS loading buffer was added and the samples were heated at 100°C for 10 min followed by immunoblot analysis.

Proteinase K protection assay

This was described before (Zhang et al., 2015). In brief, the cells were harvested and lysed in HB1 buffer (20 mM HEPES-KOH, pH 7.2, 400 mM sucrose, 1 mM EDTA) with 0.3 mM DTT and protease inhibitors by passing through a 22G needle. The lysate was centrifuged at 1000xg for 10 min and the supernatant was ultra-centrifuged at 100,000xg for 40 min to collect the total membrane pellet. The pellet was suspended with 250 μ L 35% Optiprep diluted in B88 buffer (20mM HEPES (pH 7.2), 250 mM sorbitol, 150mM potassium acetate, 5mM magnesium acetate) and layered sequentially with 700 μ L 30% Optiprep diluted in B88 and 50 μ L B88 buffer, and ultra-centrifuged at 150,000 xg for 2h. The membrane fraction floating on the top was collected and divided into three fractions (without proteinase K, with proteinase K (15 μ g/ml), and with proteinase K and 0.5% Triton X-100) 30 μ L per fraction. The reactions were performed on ice and stopped by adding PMSF and 3 \times SDS loading buffer. The samples were immediately heated at 100°C for 10 min.

Crosslink assays, immunoprecipitation, GST pull-down and immunoblot

For the DHFR assay to identify IL-1 β translocation complex, the cells expressing mL-1 β -DHFR were treated with control or aminopterin as indicated before (Zhang et al., 2015). DSP crosslink was performed (For the DSP crosslink cells were suspended in PBS with 2mM DSP at room temperature for 30 min. The reaction was quenched with 100 mM Tris (pH 7.4)). After crosslink, the membrane fraction was collected via a membrane flotation assay as indicated previously (Zhang et al., 2015). The membrane fractions were lysed and immunoprecipitation was performed with anti-FLAG beads. Samples were eluted off of the beads via FLAG peptide competition. Semiquantitative mass spectrometry was performed in Taplin Biological Mass Spectrometry Facility at Harvard Medical School.

For DSS crosslink assays, the cells or proteoliposomes were suspended in PBS with the indicated concentration of DSS at room temperature for 30 min. The reaction was quenched with 20 mM Tris followed by sample preparation for immunoblot as described before (Ge et al., 2008, 2011).

For coIP, the detail was described before (Zhang et al., 2015). Briefly, the cells were lysed on ice for 30 min in IP buffer (50 mM Tris/HCl pH 7.4, 150 mM NaCl, 1 mM EDTA, 0.5% NP40, 10% glycerol) with protease inhibitor mixture, and the lysates were cleared by centrifugation. The resulting supernatants were incubated with indicated agaroses and rotated at 4°C for 3hs. Then the agaroses were washed five times with IP buffer followed by immunoblot. For the immunoprecipitation performed after crosslinking, a similar procedure was carried out using another IP buffer (PBS, 1% NP40, 1% deoxycholate, 5mM EDTA and 5mM EGTA).

For GST pull-down, the proteins were purified and the GST-tagged bait was incubated with GSH-agarose (GE) (which was blocked by 5% milk) in IP buffer used for coIP, and rotated at 4°C for 1h. Then the beads loaded with the bait were collected and incubated with the prey protein 4°C for 2hs. The beads were washed 3 times followed by immunoblot.

Immunofluorescence, Duolink PLA and fluorescence complementation

Immunofluorescence was described previously (Zhang et al., 2015). In brief, the cells were permeabilized with 40 $\mu\text{g/ml}$ of digitonin diluted in PBS on ice for 5 min, washed once with cold PBS and immediately incubated with 4% cold paraformaldehyde for 20 min at room temperature. The cells were further permeabilized with 0.1% Triton X-100 diluted in PBS at room temperature for 10 min followed by blocking with 10% FBS diluted with PBS for 1 h and primary antibody incubation for 1 h. Cells were washed three times with PBS, followed by secondary antibody incubation for 1 h at room temperature. Fluorescence images were acquired using the Olympus FV3000 confocal microscope. Quantification was performed using ImageJ.

Duolink PLA kit was purchased from Sigma and the assay was performed according to the product manual. In brief, equal amounts of IL-1 β s-FLAG and TMED10-V5s were expressed in U2OS cells. The cells were fixed with 4% paraformaldehyde for 20 min and permeabilized with 0.1% Triton X-100 diluted in PBS at room temperature. The cells were blocked, incubated with primary antibodies and PLA probes followed by ligation and amplification using the recommended conditions according to the manual. Images were captured by Olympus FV3000 confocal microscope and quantifications were based on number of $> 1 \mu\text{m}^2$ puncta (in area) per cell using ImageJ software.

For fluorescence complementation, the cells expressing IL-1 β -GFP11 and GFP(1-10)-TMED10 were treated as indicated in each figure. The GFP signal in the cells was collected by CytoFlex LX (Beckman) and analyzed by Flowjo software.

Cryosectioning, immunolabeling and electron microscopy

We followed the Tokuyasu method as described previously (Slot and Geuze, 2007). Cells were fixed in 2% formaldehyde and 0.01% glutaraldehyde in PB buffer at 4°C overnight and then washed with chilled PB /Glycine. The cells were scraped from the bottom of the plastic dishes in 1% gelatin of PB buffer, centrifuged at 1000rpm/min for 2min and suspended in 12% gelatin at 37°C for 10min. The gelatin-cell mixture was solidified on ice for 15min. Small blocks about 0.5mm³ were made and immersed in 2.3M sucrose overnight at 4°C. Cryosections of 70nm were made at -120°C with an ultratome (Leica EM FC7). After sections were thawed at room temperature, immunolabeling was performed with mouse anti-FLAG and rabbit anti-GFP antibodies followed by immune-Gold secondary antibody. The sections were treated with methyl cellulose/uranyl acetate and subsequently imaged under the H-7650 80kv transmission electron microscope.

Analysis of Serum IL-1 β and gene expression level

Serum IL-1 β was analyzed by ELISA using Mouse IL-1 β Uncoated ELISA kit (Thermo). Gene expression was determined by qRT-PCR. Total RNA was isolated and cDNA was generated using retrotranscription. The samples were amplified using a CFX-96 machine (Bio-Rad) and SYBR Green master mix (TSINGKE, China) according to the manufacturer's instructions; data were normalized to the GAPDH control. The sequences of the primers for were listed in [Key Resources Table](#).

All-atom (AA) molecular dynamics (MD) simulations

The dynamic binding processes of TMED10 cytoplasmic part (sequence: YLRFFKAKKLIE) and designed peptide motifs were studied by AAMD simulations with CHARMM36m force field (Huang et al., 2017). The atomic structures of these peptides were predicted via I-TASSER web server (Yang et al., 2015), and the initial binding poses between them was obtained using ZDOCK protein docking (Pierce et al., 2011). Then, the docking complex was put in a simulation water box with 150 mM NaCl with CHARMM-GUI webserver (Lee et al., 2016a). Following by the 10 ns pre-equilibration processes, the final 200 ns production runs were performed with GROMACS software (version 2016.5) (Pronk et al., 2013) with the time step of 2 fs.

QUANTIFICATION AND STATISTICAL ANALYSIS

The ways of quantification of each experiment have been provided in the [Method Details](#). The statistical information of each experiment, including the statistical methods, the P values and numbers (n), were shown in the figures and corresponding legends. Statistical significance for gene expression, serum IL-1 β level, imaging quantification and molecular dynamics simulations was determined using two-tailed t test. For survival comparison, the logrank test was employed. Statistical analyses were performed in GraphPad Prism.

DATA AND CODE AVAILABILITY

This study did not generate any unique datasets or code.

ADDITIONAL RESOURCES

This study did not generate any additional resources.

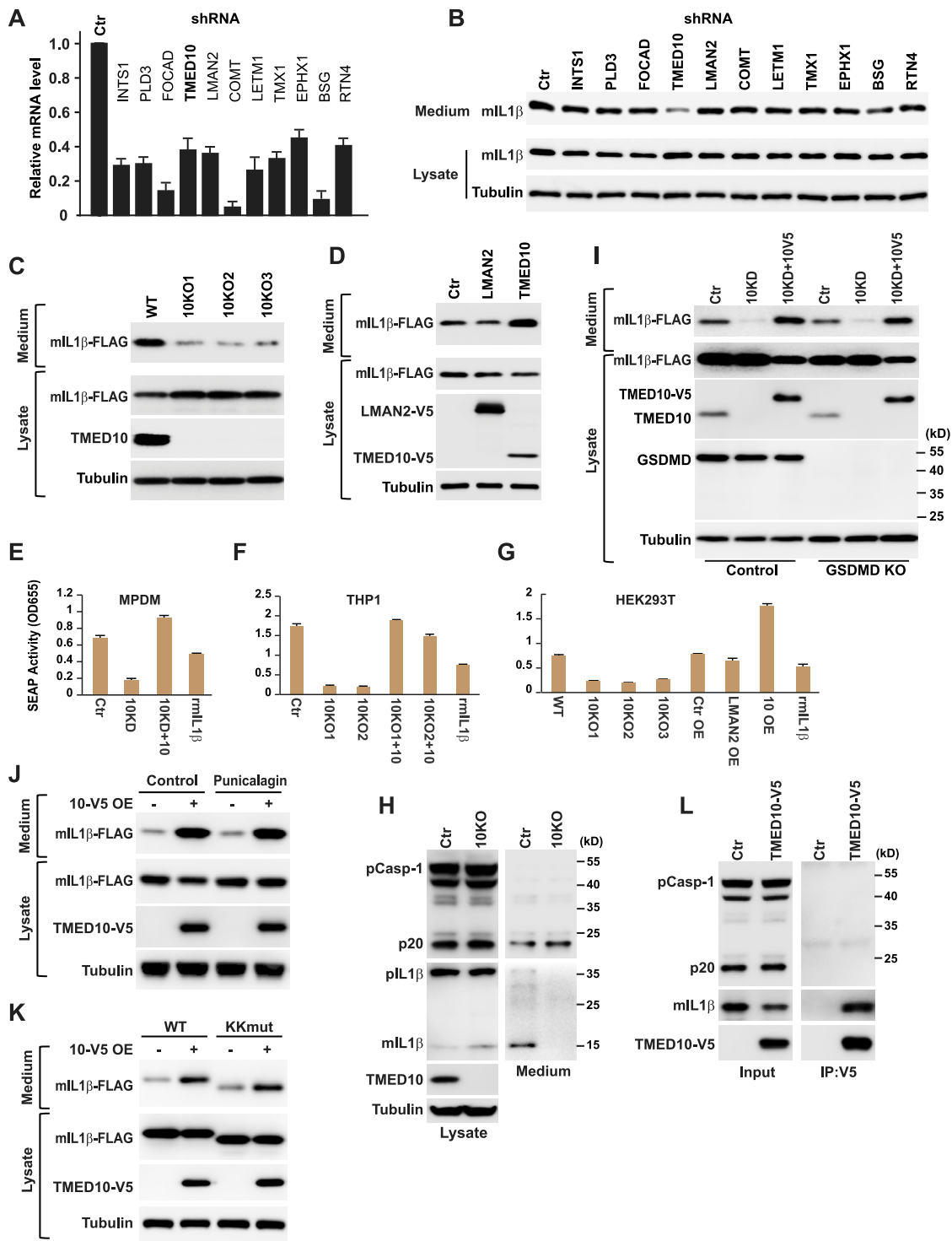


Figure S1. TMED10 Regulates mIL-1β Secretion, Related to Figures 1 and 2

(A and B) HEK293T cells were co-transfected with mIL-1β plasmid and indicated shRNA plasmids. 72h post transfection, the cells were harvested for knockdown efficiency test by Q-PCR (A) or mIL-1β secretion (B).

(C) Secretion of mIL-1β in control or three TMED10 KO HEK293T lines.

(D) Secretion of mIL-1β in HEK293T with control, LMAN2-V5 and TMED10-V5 expression.

(E-G) HEK-Blue IL-1β cells (InvivoGen) were treated with culture medium derived from indicated cells and treatments, or with 0.1 μg/ml recombinant mIL-1β as a standard. Levels of SEAP which indicate IL-1β activity in the medium were monitored using QUANTI-Blue.

(legend continued on next page)

(H) Secretion of Caspase 1 p20 and mL-1 β in WT and TMED10-KO THP-1 cells after LPS and ATP treatment.

(I) Secretion of mL-1 β in control or GSDMD-KO HeLa cells with control, TMED10-KD or TMED10 expression after KD.

(J) Secretion of mL-1 β in HEK293T transfected with mL-1 β -FLAG plasmid alone or together with TMED10-V5 plasmid with or without punicalagin.

(K) Secretion of WT-mL-1 β or KK mutant-mL-1 β by HEK293T transfected with mL-1 β -FLAG (WT or KK mutant) plasmids alone or together with TMED10-V5 plasmid.

(L) CoIP performed using TMED10-V5 expressing THP-1 to determine TMED10, mL-1 β and caspase 1 association after LPS and ATP treatment.

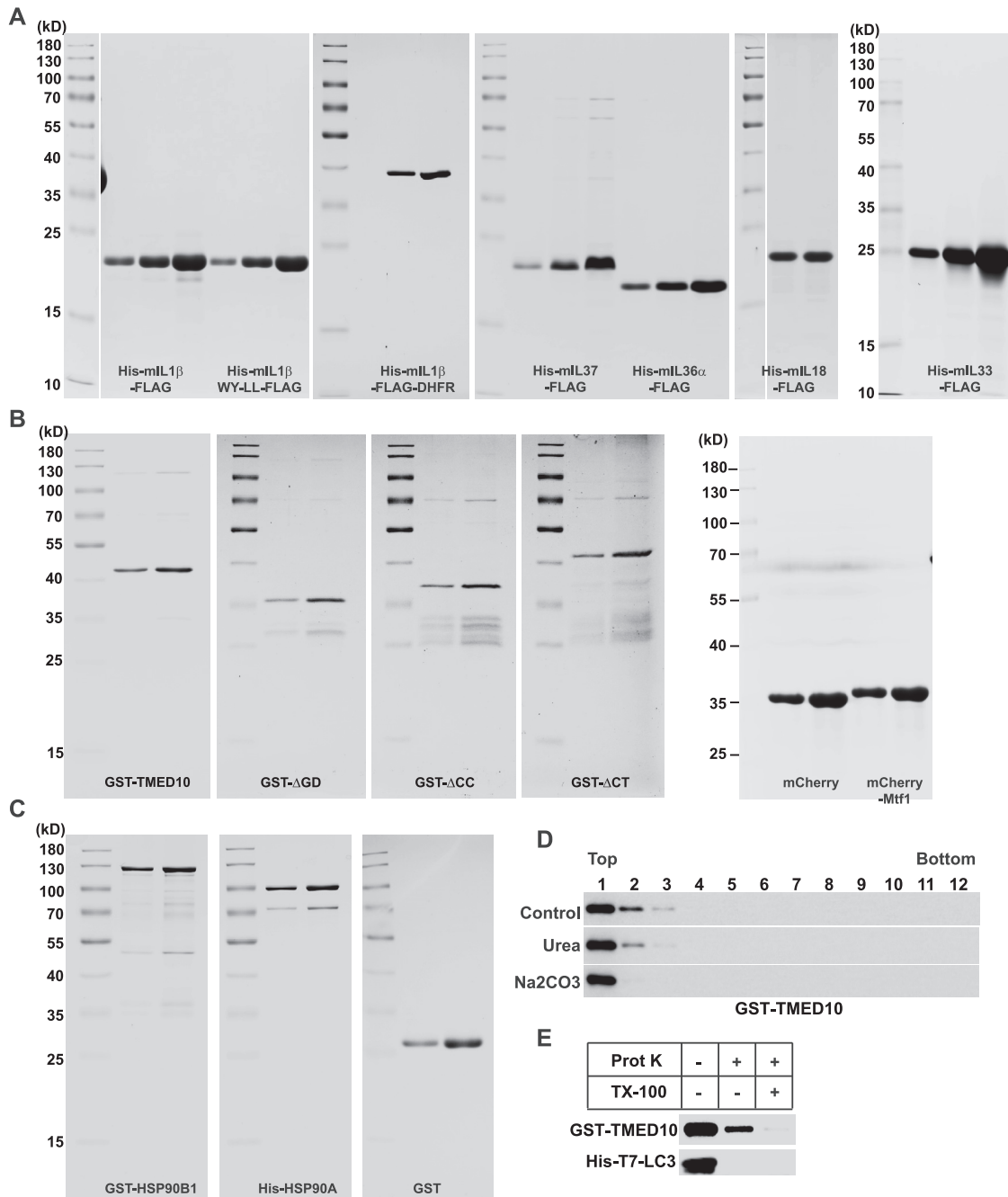


Figure S2. Coomassie Blue Staining of the Purified Protein and Proteoliposome Validation, Related to Figures 2, 4, and 5

(A–C) Indicated proteins were purified from *E. coli*. Two or three concentrations of the purified proteins were loaded onto the gels. The images for mIL-1 β , mIL-18, and mCherry were cropped from whole gels with protein bands irrelevant for the experiments shown in the manuscript.

(D) TMED10 proteoliposomes were treated with control buffer, with 2M Urea or 0.25M Na₂CO₃ (PH 11). A membrane flotation assay was performed to analyze the membrane-bound TMED10 after each treatment.

(E) Proteinase K protection assay performed with TMED10 proteoliposomes.

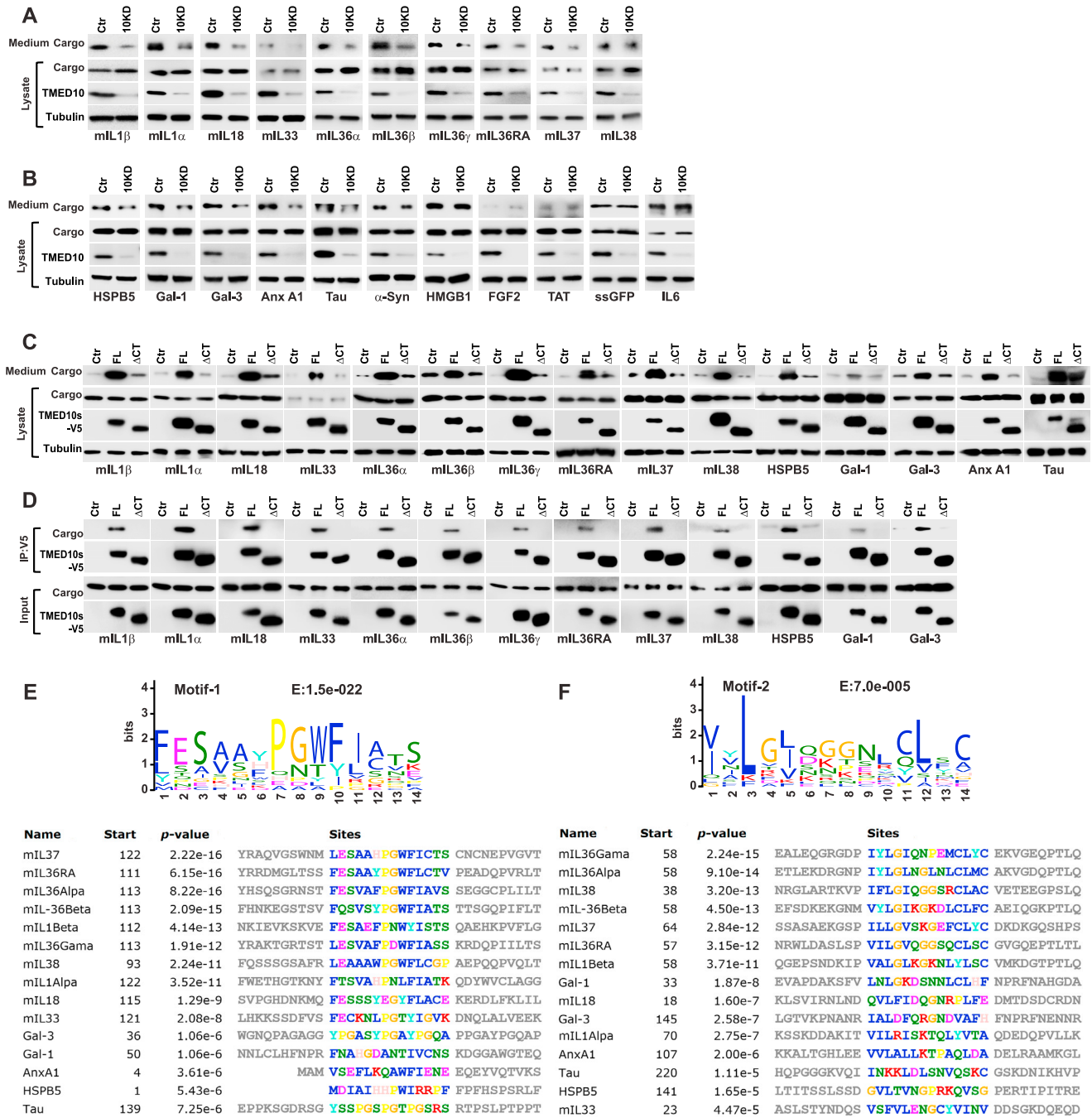


Figure S3. Immunoblot Showing the Effect of TMED10 on the Secretion of the Indicated Cargoes, Related to Figure 3

(A and B) Secretion of mature interleukin-1 s (A) and other indicated cargoes (B) in control and TMED10 KD HEK293T.

(C) Secretion of indicated cargoes in control, TMED10 or TMED10ΔCT-expressing HEK293T.

(D) CoIP performed to determine the association of TMED10 and TMED10ΔCT with the indicated cargoes.

(E and F) The sequence and position of motif-1 (E) and motif-2 (F) in the indicated cargoes. For the interleukin-1 s, the position of motifs is provided according to the mature form.

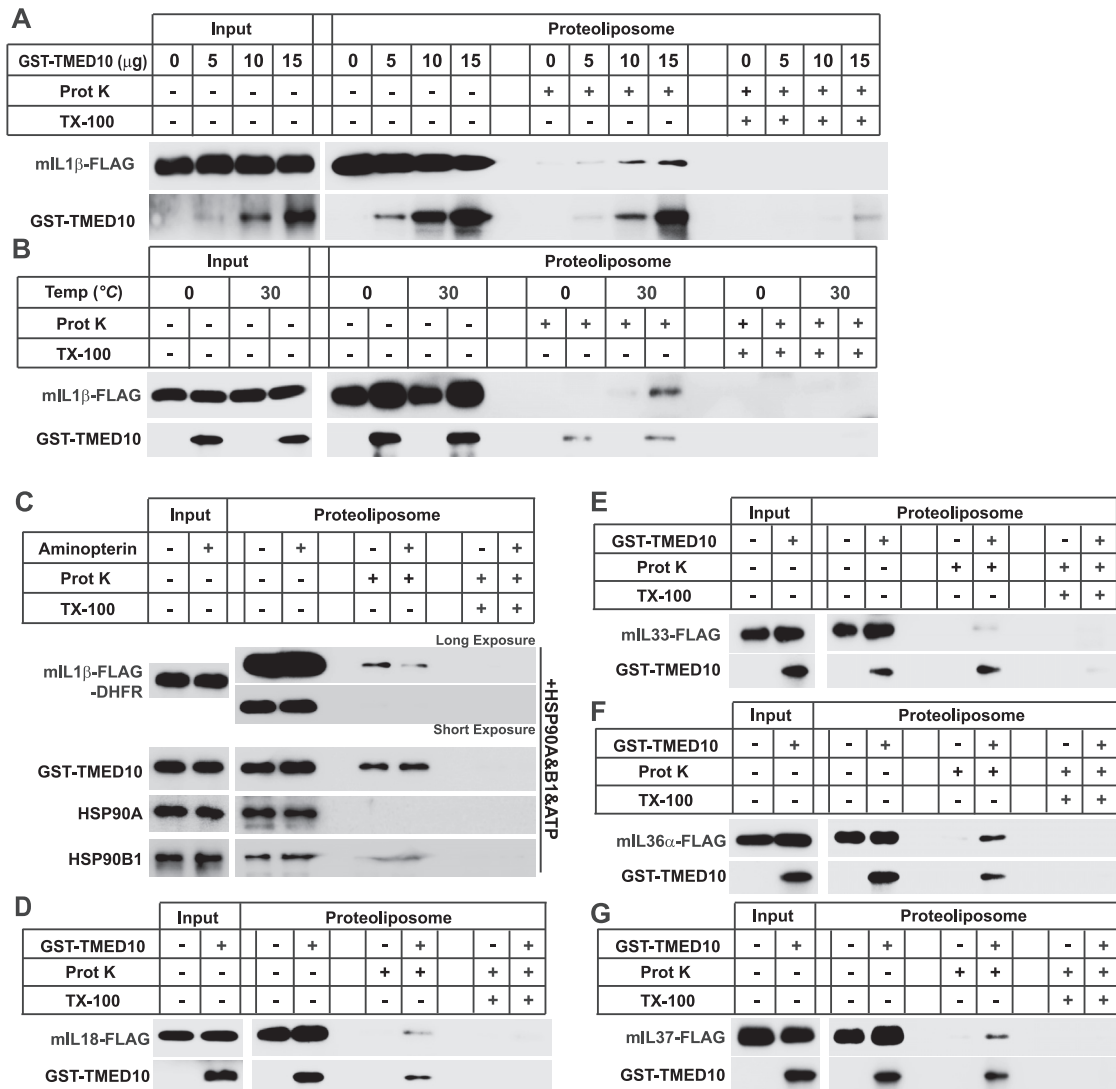


Figure S4. Membrane Translocation Interleukin 1 s, Related to Figures 4 and 5

(A) *In vitro* translocation of mIL-1 β with control or liposomes with increasing GST-TMED10.

(B) The *in vitro* translocation assay with control or GST-TMED10 liposomes performed at the temperature of 0 $^{\circ}$ C and 30 $^{\circ}$ C.

(C) *In vitro* membrane translocation assay with GST-TMED10 proteoliposomes, mIL-1 β -DHFR, HSP90s, and ATP in the absence or presence of aminopterin.

(D–G) *In vitro* translocation assay with control or GST-TMED10 liposomes performed with mIL-18 (D), mIL-33 (E), mIL-36 α (F) and mIL-37 (G).

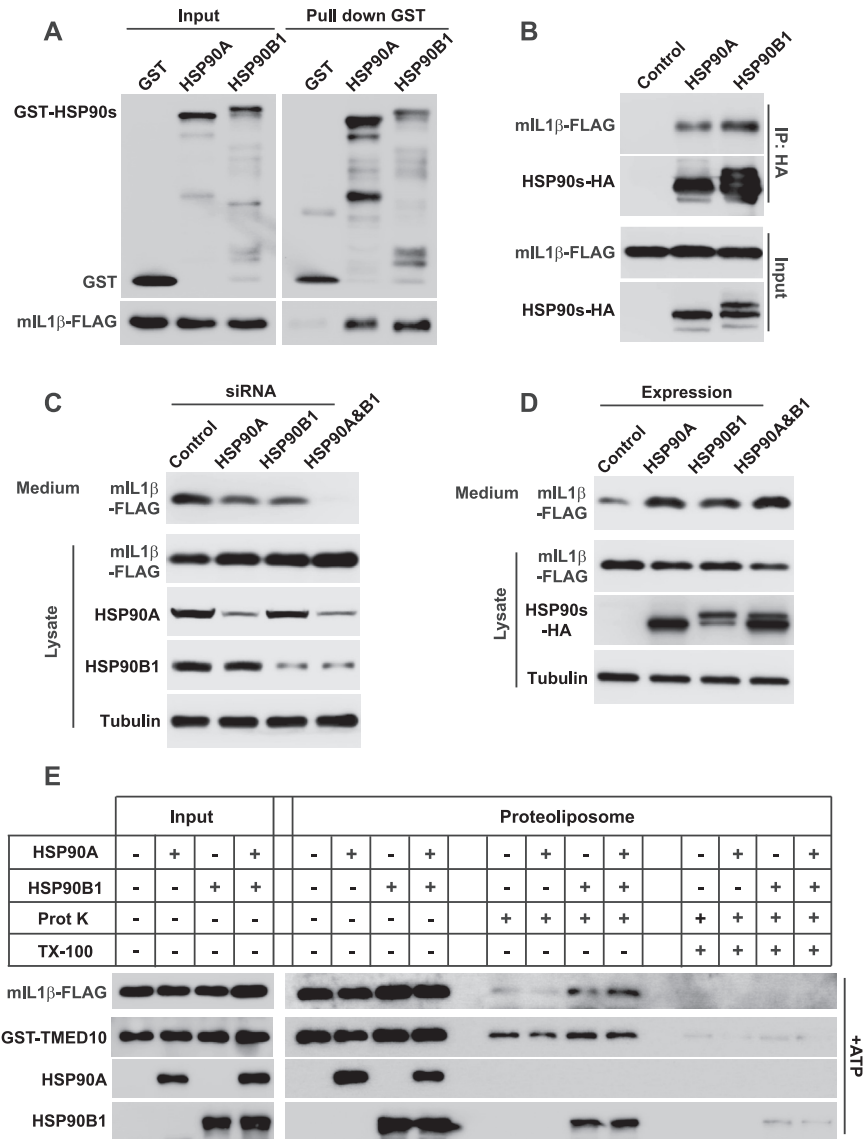


Figure S5. HSP90A and HSP90B1 Promotes TMED10-Mediated Membrane Entry of mIL-1β, Related to Figure 4

(A) A GST pull-down experiment showing the interaction of HSP90A and HSP90B1 with mIL-1β

(B) CoIP performed using HEK293T with mIL-1β or together with HSP90A or HSP90B1.

(C) mIL-1β secretion in HEK293T with control, HSP90A, HSP90B1 or both KD.

(D) mIL-1β secretion in HEK293T with control, HSP90A, HSP90B1 or both expression.

(E) TMED10 proteoliposomes and TMED10-HSP90B1 proteoliposomes (HSP90B1 incorporated in the lumen) were generated. *In vitro* mIL-1β membrane translocation assay was performed with the proteoliposomes in the presence or absence of HSP90A plus ATP.

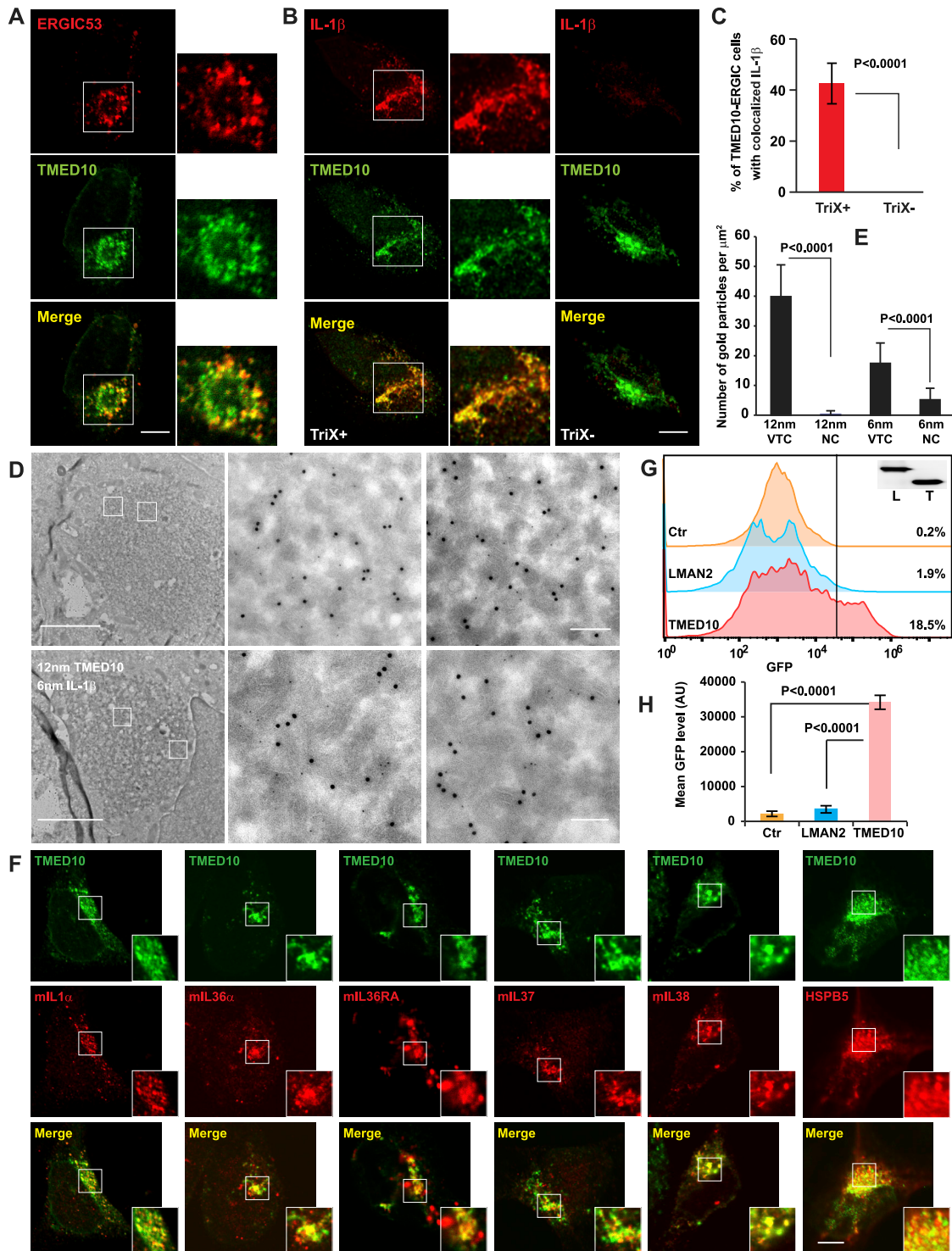


Figure S6. Cargoes Enter into the TMED10-Positive Membrane Compartment, Related to Figure 6

(A) Immunofluorescence of U2OS expressing TMED10-V5 with the anti-ERGIC53 antibody. Bar: 10 μm .

(B) U2OS expressing TMED10-V5 and mIL-1 β -FLAG were treated with cold digitonin (40 $\mu\text{g}/\text{ml}$), fixed and either non-treated (TriX-) or permeabilized with 0.1% Triton X-100 to enable staining luminal proteins. Immunofluorescence was performed. Bar: 10 μm .

(C) Quantification of the percentage of mIL-1 β localized with TMED10-V5-positive ERGIC. The graph represents mean \pm SD. P values are indicated (two-tailed t test, n = 6).

(D) Immuno-EM of U2OS expressing TMED10-EGFP and mIL-1 β -FLAG (TMED10, 12nm, mIL-1 β , 6nm, bar: 1 μm in overview and 100 nm in the zoomed in).

(legend continued on next page)

(E) Quantification of immune-gold labeling specificity. U2OS with mL-1 β -FLAG and TMED10-EGFP expression as well as a negative control (NC) without the expression of these proteins were labeled with antibodies as shown in (D). Electron microscopy images positive for the vesicular-tubular compartment (VTC) from cells with mL-1 β -FLAG and TMED10-EGFP, and cell images from NC cells were acquired and gold particles in each image were counted and normalized to particles/ μm^2 . The graphs represent mean \pm SD. P values are indicated (two-tailed t test, n = 37 images for 12 nm & 6 nm VTC, n = 83 images for 12 nm & 6 nm NC, for each group).

(F) Immunofluorescence of U2OS expressing TMED10-V5 together with indicated cargoes. Bar: 10 μm .

(G and H) Control or U2OS expressing GFP(1-10)-TMED10 or GFP(1-10)-LMAN2 were transfected with mL-1 β -GFP11. FACS analysis was performed to determine the complemented GFP signal. (F) Histogram of GFP signal; (G) Quantification of GFP signal. Error bars indicate standard deviation of three independent experiments. The graph represents mean \pm SD. P values are indicated (two-tailed t test, n = 3).

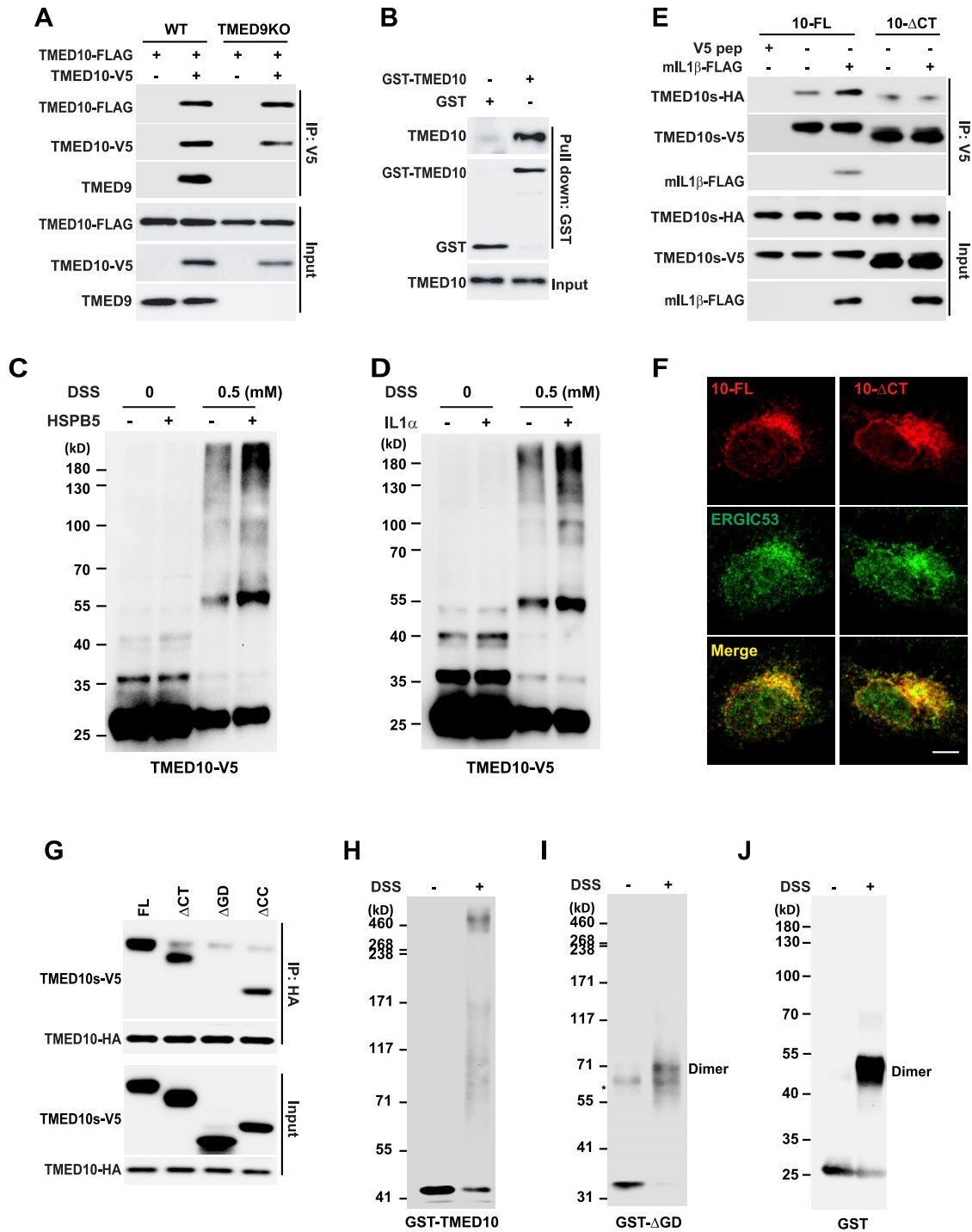


Figure S7. GOLD Domain of TMED10 Is Required for Oligomerization, Related to Figure 7

(A) CoIP performed using control and TMED9-KO U2OS cells expressing TMED10-FLAG alone or with TMED10-V5.

(B) GST pull-down with GST, GST-TMED10 and TMED10 proteins.

(C) A crosslink assays performed using HEK293T with TMED10-V5 alone or together with HSPB5 expression.

(D) A crosslink assays performed using HEK293T with TMED10-V5 alone or together with mL1- α expression.

(E) CoIP performed using TMED10-KO HEK293T expressing TMED10-HA and TMED10-V5 or TMED10 Δ CT-HA and TMED10 Δ CT-V5 without or with mL1- β expression.

(F) Immunofluorescence of U2OS cells with TMED10-V5 or TMED10 Δ CT-V5 using antibodies against V5 and ERGIC53. Bar: 10 μ m

(G) CoIP performed using TMED10 KO HEK293T with TMED10-HA expression together with indicated TMED10-V5 variants.

(H–J) Crosslink assays performed using GST-TMED10 proteoliposomes (H), GST-TMED10 (Δ GD) proteoliposomes (I) or GST (J).